DOI:
10.1109/TFUZZ.2023.3323650

Document Version
Peer reviewed version

Citation for published version (APA):
Li, X., Wang, X., Liu, F., Lam, H-K., & Du, Y. (2023). Stability Analysis and Event-Triggered Control for IT2 Discrete-time Positive Polynomial Fuzzy Networked Control Systems with Time Delay. *IEEE Transactions on Fuzzy Systems*. https://doi.org/10.1109/TFUZZ.2023.3323650

Stability Analysis and Event-Triggered Control for IT2 Discrete-time Positive Polynomial Fuzzy Networked Control Systems with Time Delay

Xiaomiao Li, Xiaoxiao Wang, Fucai Liu, Hak-Keung Lam, *Fellow, IEEE*, and Yuehao Du

***Abstract*—This paper investigates the stability analysis and event-triggered controller design of interval type-2 (IT2) discrete-time positive polynomial fuzzy networked control (DPPFNC) systems with time delay subject to asynchronous premises. The reasonable design of the IT2 polynomial fuzzy event-triggered controller guarantees the closed-loop system's positivity and stability, reduces energy consumption and efficiently utilizes the communication bandwidth. Furthermore, for DPPFNC systems with time delay, obtaining more relaxed stability conditions and lower network communication frequency is quite challenging, even for the current advanced theory. Meanwhile, to strengthen the practicality of the control strategy, the asynchronous constraints of premise variables due to the introduction of the network are considered. Aiming at the above problems, a polynomial fuzzy event-triggered control strategy is proposed based on the stability analysis of IT2 membership-function-dependent (IT2-MFD) and imperfect premise matching (IPM). First, the IT2 polynomial fuzzy model, which employs IT2-MFs to capture parameter uncertainty, depicts the event-triggered positive nonlinear dynamics. Second, an IT2 polynomial fuzzy event-triggered controller is designed by introducing the 1-norm event-triggered control (ETC) strategy. Then, by optimizing the approximation error between the original and the approximate membership function, a genetic algorithm (GA) is employed to relax the stability criteria. Finally, numerical and practical examples illustrate the viability of the suggested design.**

***Index Terms*—Discrete-time positive polynomial fuzzy networked control (DPPFNC) systems, event-triggered control (ETC) design, sum-of-squares (SOS), interval type-2 membership function dependent (IT2-MFD) method, Genetic Algorithm membership functions (GA-MFs).**

I. Introduction

POSITIVE networked control systems (PNCSs) are regarded as promising sharing communication network systems due to their benefits, including low prices, easy installation and maintenance [1], [2]. Positive networked control systems have both the complex dynamic behaviours of general networked control systems (NCSs) [3], [4] and the unique properties of positive systems, that is, their states are defined in the positive quadrant conical space rather than the whole space [5]. The typical applicable examples for such systems can be found in a broad range of areas [6], [7]. The work [6] established positive dynamics for the smart grid's agent-level power distribution remote monitoring procedure. In [7], a susceptible-exposed-infected-removed (SEIR) positive network system model was constructed, and an ETC framework was presented to contain the transmission process. In addition, in most PNCSs, all sampled data (SD) must be transmitted over a shared communication network, which is a typical time-triggered control scheme [8]. However, when dealing with PNCSs with limited resources, some scattered fluctuations of SD in the PNCSs will cause more interference to the controller execution process. Therefore, to reduce unnecessary SD transmission and save limited network bandwidth, the ETC [9], [10] and self-triggered control strategies [11] have attracted much interest. On this basis, the transmission delay caused by communication network insertion is considered.

Since most NCSs in actual production are complex and nonlinear, it is difficult to establish accurate models of control plants. Therefore, the fuzzy control theory of nonlinear systems emerged [12]. When dealing with nonlinear systems utilizing fuzzy reasoning, the T-S fuzzy framework [13], [14] can be a practical instrument, and some relevant results such as output feedback [15], tracking control [16] and fuzzy stabilization [17] were reported. Besides, a polynomial fuzzy model [18] was recently proposed, which allows polynomials to appear in fuzzy consequences and represents a broader range of nonlinear systems. [19] employed polynomial fuzzy modelling on the lipoprotein breakdown and the potassium-ions transport system, and designed a controller for treatment to stabilize the patient's self-metabolic function. Recently, polynomial fuzzy control frame is successfully applied to complex nonlinear NCSs under the ETC strategy. For example, in [20], considering the limited bandwidth communication in the network environment, a design methodology for IT2 event-triggered polynomial controllers in NCSs is advanced. From [21], a novel ETC strategy is applied to make the stochastic fuzzy singular systems admissible, extended dissipative and save the network resources. However, due to the limitations of positive constraints, the research of ETC design for PNCSs has become challenging.

Most existing PNCS systems employs type-1 fuzzy logic frame [22], but the type-1 fuzzy set cannot directly address

The Natural Science Foundation with Project 62103356, the Natural Science Foundation of Hebei Province with Project (F2021203069, F2022203043), the Science and Technology Project of Hebei Education Department with Project BJK2022040 and the Oversea Talents of Hebei Province Foundation with Project C20210319 all provided funding in support of this work. *(Corresponding Author: H.K. Lam)*

Xiaomiao Li, Xiaoxiao Wang, Fucai Liu, and Yuehao Du are with the Key Lab of Industrial Computer Control Engineering of Hebei Province, Yanshan University, Qinhuangdao 066004, Hebei Province, China. (e-mail: xsm760595299@163.com; wxx19980401@163.com; lfc@ysu.edu.cn; godofhouston@163.com).

H.K. Lam is with the Department of Engineering, King's College London, Strand, London WC2R 2LS, United Kingdom. (e-mail: hak-keung.lam@kcl.ac.uk).

some uncertain problems. Type-2 fuzzy sets [23], which have been demonstrated in applications like inverted pendulum control [24], extended Kalman filters [25], and nonlinear control [26], have been proposed to capture the uncertainty accurately. However, this framework significantly increases the computational complexity, making obtaining the computational results challenging. Depending on the type-2 fuzzy framework, the interval type-2 (IT2) fuzzy framework theory was created to address this drawback, and the secondary membership degree was set to 1. Benefitting from an excellent property for describing uncertain nonlinearities inspired by [27], the IT2 fuzzy ETC controller is adopted, the stability criterion of SOS method is proposed in [20]. However, for some NCSs with particular positive constraints, the papers about IT2 fuzzy ETC are no longer applicable, which is one of the motivations of this study.

In terms of the control design paradigm, the popular parallel distributed compensation (PDC) technique favours stability analysis [28] as the existence of crossed terms. But, the PDC design framework assumes that the model and the controller have the equivalent rule number and premise MFs. Considering the parameter uncertainties [29] and the existence of ETC schemes, it is impossible to design event-triggered fuzzy controllers that can stabilize IT2 fuzzy model using the PDC technique. In addition, since the event-triggered fuzzy controller can only observe the sampled state after triggering action, the MFs of the controller and the model are not one-to-one corresponding. For the above problems, an imperfect premise matching (IPM) [30] design framework is employed. It allows fuzzy rules and MFs's shapes to be more complex and asymmetric and increases the usability of the controller.

It has been demonstrated in [30] that adopting a MFD approach is crucial in relaxing system stability criteria. For specific MFs, the MFD-based stability criteria are accurate and relaxed. In literature [31], [32], more information about MFs is introduced into stability analysis by using approximated MFs methods, for instance, piecewise-linear MFs (PLMFs) [31], Taylor series MFs (TSMFs) [32] et al. It is not difficult to find that the above approximation methods are all interpolation methods, interpolation functions use approximation order to describe the quality of approximations. However, the global approximation error cannot be reduced even if the approximation order is very high because of the Runge phenomenon [33]. So, this paper introduces the uniform norm in the space, and the quality of the approximation is controlled by the defined norm with a genetic algorithm (GA), which can effectively avoid the situation that the approximation is good at individual points but the overall approximation is very poor [34]. GA is an optimization mechanism proposed by Professor Holland [35] to imitate the natural selection and evolution mechanism of "survival of the fittest" in nature. A fundamental principle of GA is to simulate the biological processes required for evolution to reflect the survival of the fittest and maintain artificial ecosystems [36]. Ingeniously, the optimum approximation polynomial of the IT2 MFs is solved in this paper using GA, which has the consequence of relaxing the stability conditions.

The polynomial fuzzy ETC strategy mentioned in this paper can be applied to the smart grid's agent-level power distribution system to realize the real-time accuracy of information transmission in the network channel. In the SEIR dynamic epidemic model, the 1-norm event-triggered condition designed in this paper can realize limited isolation and further control the SEIR epidemics. Aiming at the above difficulties and problems, the items that follow belong to the thesis's contributions:

1) Considering the nonlinearity parameters uncertainty and the unique positivity constraint in the network environment, the dynamics of DPPFNC systems with asynchronous premises are proposed to be modelled using an *IT2 polynomial fuzzy model with time delay*. Advanced polynomial fuzzy models, relative to T-S fuzzy models, allow the existence of polynomials in subsystems while considering the adverse effects of excessive communication burden and inherent time delay, making the system model more comprehensive than existing results.
2) To reduce the network resource consumption and facilitate remote control of the DPPFNC systems with time delay, *an IT2 polynomial fuzzy ETC strategy* with the IPM technology is proposed, which allows the open-loop system and controller to have different premise variables. A more reasonable *1-norm event-triggered condition* is created, and the influence of ETC on stability domain and system performance is delivered.
3) A novel IT2-MFD analysis method is presented to approximate the IT2-MFs by *GA-MFs*. Based on the optimum uniform approximation theory, the approximate errors in terms of minimized uniform norm are further brought in, reducing the conservativeness of stability analysis.

The remainder of this essay is structured as follows. Networked IT2 polynomial fuzzy model, ET controller, as well as the ETC scheme are briefly represented in Section II. In Section III, basic and IT2-MFD stability derivation with GA-MFs for event-trigger-based DPPFNC system are carried out to generate relaxation stability conditions. Section IV gives numerical and practical examples to verify the analysis results. The conclusion is presented in section V.

II. Notations and Preliminaries

A. Notation

With the vector $\mathbf{x}(t)=[x_1(t),x_2(t),...,x_n(t)]^T$, $\|\mathbf{x}(t)\|_1=\sum_{i=1}^n|x_i(t)|$ and $\|\mathbf{x}(t)\|_\infty=\max\limits_{1\le i\le n}|x_i(t)|$ are the 1-norm and ∞ norm of $\mathbf{x}(t)$. Define $\mathbf{1}_n=(1,1,...,1)^T\in\Re^n$, $\mathbf{1}_{n\times n}$ denotes an $n\times n$ dimensional matrix whose elements are all 1. $\mathbf{Q}>0$ (<0) indicates $\mathbf{Q}$ is a positive (negative) definite matrix, $\mathbf{Q}\succ 0$ ($\prec 0$) means that all elements in $\mathbf{Q}$ are positive (negative). G^+ and G^- represent the non-negative and non-positive components of matrix G, satisfying $G^+\succ 0, G^-\prec 0$, respectively. $\underline{n}=\{1,2,...,n\}, \underline{p}=\{1,2,...,p\}, \underline{\Psi}=\{1,2,...,\Psi\}, \underline{c}=\{1,2,...,c\}, \underline{\Omega}=\{1,2,...,\Omega\}, \underline{L}=\{1,2,...,L\}$ represents the order of fuzzy model, the rule number of fuzzy model, the number of premise variable of fuzzy model, the rule number of controller, the number of premise variable of controller, the number of connected operating subdomain in $\boldsymbol{\Psi}$, where $n, p, \mathit{\Psi}, c, \Omega, L \in \mathbb{Z}^+$, respectively.

B. Time Delay Discrete-time IT2 Polynomial Fuzzy Model

p-rule discrete-time IT2 polynomial fuzzy models are presented to describe nonlinear objects with uncertainty. IT2 fuzzy sets explain the antecedent, and a polynomial dynamic system provides the consequent. The structure of the i^{th} rule is as follows:

$$\begin{aligned}&\text{Rule } i: \text{IF } f_1(\mathbf{x}(k)) \text{ is } \tilde{M_1^i} \text{ AND} \cdots \text{AND } f_{\mathit{\Psi}}(\mathbf{x}(k)) \text{ is } \tilde{M_{\mathit{\Psi}}^i}\\ &\text{THEN } \mathbf{x}(k+1) = \mathbf{A}_i(\mathbf{x}(k))\mathbf{x}(k)\\ &\qquad + \mathbf{A}_{\tau i}(\mathbf{x}(k))\mathbf{x}(k-\tau) + \mathbf{B}_i(\mathbf{x}(k))\mathbf{u}(k_\wp),\end{aligned} \tag{1}$$

$$\mathbf{x}(k)=\psi(k), \qquad k = [-\tau, 0] \tag{2}$$

in which $\mathbf{x}(k) \in \Re^n$, $\mathbf{u}(k_\wp) \in \Re^m$ and $\psi(k) \in \Re^n$ are the system state, control input and initial condition, respectively; $\tilde{M_\alpha^i}$ is the IT2 fuzzy set of premise variable $f_\alpha(\mathbf{x}(k))$ under the i^{th} rule, $i \in \underline{p}$, $\alpha \in \underline{\mathit{\Psi}}$; $\mathbf{A}_i(\mathbf{x}(k)) \in \Re^{n\times n}$, $\mathbf{A}_{\tau i}(\mathbf{x}(k))\mathbf{x}(k-\tau) \in \Re^{n\times n}$ and $\mathbf{B}_i(\mathbf{x}(k)) \in \Re^{n\times m}$ are the defined polynomial system, time delay and input matrices.

The next interval sets describe the firing strength under the i^{th} rule:

$$W_i(\mathbf{x}(k)) = \left[w_i^L(\mathbf{x}(k)), w_i^U(\mathbf{x}(k))\right], \qquad \forall i. \tag{3}$$

$w_i^L(\mathbf{x}(k)) = \prod_{\alpha=1}^{\mathit{\Psi}} \underline{\mu}_{\tilde{M}_\alpha^i}(f_\alpha(\mathbf{x}(k)))$ and $w_i^U(\mathbf{x}(k)) = \prod_{\alpha=1}^{\mathit{\Psi}} \bar{\mu}_{\tilde{M}_\alpha^i}(f_\alpha(\mathbf{x}(k)))$ represent the lower and upper grades of membership, respectively. $\underline{\mu}_{\tilde{M}_\alpha^i}(f_\alpha(\mathbf{x}(k))) \geq 0$ represent the lower MFs, $\bar{\mu}_{\tilde{M}_\alpha^i}(f_\alpha(\mathbf{x}(k))) \geq 0$ represent the upper MFs. Furthermore, it exhibits the property that $0 \leq \underline{\mu}_{\tilde{M}_\alpha^i}(f_\alpha(\mathbf{x}(k))) \leq \bar{\mu}_{\tilde{M}_\alpha^i}(f_\alpha(\mathbf{x}(k))) \leq 1$, so $0 \leq w_i^L(\mathbf{x}(k)) \leq w_i^U(\mathbf{x}(k)) \leq 1$ for all i. Then the dynamics of the time delay IT2 polynomial fuzzy model are

$$\begin{aligned}\mathbf{x}(k+1) = &\sum_{i=1}^{p} \tilde{w}_i(\mathbf{x}(k))\Big(\mathbf{A}_i(\mathbf{x}(k))\mathbf{x}(k)\\ &+ \mathbf{A}_{\tau i}(\mathbf{x}(k))\mathbf{x}(k-\tau) + \mathbf{B}_i(\mathbf{x}(k))\mathbf{u}(k_\wp)\Big),\end{aligned} \tag{4}$$

in which

$$\tilde{w}_i(\mathbf{x}(k)) = \underline{\lambda}_i(\mathbf{x}(k))w_i^L(\mathbf{x}(k)) + \bar{\lambda}_i(\mathbf{x}(k))w_i^U(\mathbf{x}(k)) \geq 0, \forall i, \tag{5}$$

$$\sum_{i=1}^{p} \tilde{w}_i(\mathbf{x}(k)) = 1, \tilde{w}_i(\mathbf{x}(k)) \geq 0, \qquad \forall i. \tag{6}$$

$\tilde{w}_i(\mathbf{x}(k))$ are the grades of the embedded MFs containing only $\mathbf{x}(k)$, consistent with the premise variable $f_\alpha(\mathbf{x}(k))$, $\alpha \in \underline{\mathit{\Psi}}$, independent of the term $\mathbf{x}(k-\tau)$. Nonlinear type reduction functions $\underline{\lambda}_i(\mathbf{x}(k))$ and $\bar{\lambda}_i(\mathbf{x}(k))$ exist but not be known, for all i, owning the properties $0 \leq \underline{\lambda}_i(\mathbf{x}(k)) \leq \bar{\lambda}_i(\mathbf{x}(k)) \leq 1$ and $\underline{\lambda}_i(\mathbf{x}(k)) + \bar{\lambda}_i(\mathbf{x}(k))= 1$.

Definition 1 ([5], [37]): If the corresponding trajectory for System (1) remains in the positive orthogonal for all integer k, provided any nonnegative initial state $\mathbf{x}(0) = x_0$ and any input $\mathbf{U}(k) \succeq 0$: $\mathbf{x}(k) \in \mathbb{R}_+^n$, then System (1) is positive.

Lemma 1 ([5]): The fuzzy system $\mathbf{x}(k+1) = \mathbf{A}(\mathbf{x}(k))\mathbf{x}(k) + \mathbf{B}(\mathbf{x}(k))\mathbf{u}(k)$ is positive according to Definition 1 if and only if $\mathbf{A}(\mathbf{x}(k)) \succeq 0$ and $\mathbf{B}(\mathbf{x}(k)) \succeq 0$.

Remark 1: $\tilde{w}_i(x(k))$ is a set of infinite type-1 polynomial fuzzy models whose MFs are deterministic. Therefore, referring to the modeling process of the type-1 polynomial fuzzy model, the IT2 MFs satisfy $\sum_{i=1}^{p} \tilde{w}_i(x(k)) = 1$. When uncertain parameters exist in nonlinear systems, type-1 fuzzy sets cannot capture uncertainty information properly, while IT2 fuzzy sets effectively solve this problem.

Remark 2: As opposed to T-S fuzzy models, advanced polynomial fuzzy models allow some of the original nonlinear components to remain unchanged so that a larger range of nonlinear systems can be accurately represented with fewer fuzzy rules. Besides, monomial vector $\hat{\mathbf{x}}(\mathbf{x}(k))$ to represent polynomial fuzzy models is not unique in [20]. And employing $\mathbf{x}(t)$ instead of $\hat{\mathbf{x}}(\mathbf{x}(k))$ conducts stability analysis more straightforwardly.

C. Event-Triggered Control Scheme

The 1-norm ETC strategy is introduced for the IT2 DPPFNC system with time delay to improve communication efficiency. First, define the variable $\mathbf{e}_{k_\wp}(k)$ as following to describe the error among the update instants and the actual state after k^{th} transition:

$$\mathbf{e}_{k_\wp}(k) = \mathbf{x}(k_\wp) - \mathbf{x}(k), \tag{7}$$

$\{k_\wp\}$, $\wp \in \mathbb{N}$ denotes successful release instant set. Obviously, the transmission sequence $\{k_\wp\}$ needs to be defined as $\aleph = \{k_\wp \,|\wp \in \mathbb{N}\} \subseteq \{k\,|k \in \mathbb{N}\}$ to describe the triggering instants. Then, an event-triggered condition in the 1-norm form is applied to determine the transmission of sampled data

$$\left\|\mathbf{e}_{k_\wp}(k)\right\|_1 \leq \gamma\|\mathbf{x}(k)\|_1, \tag{8}$$

where γ is a predefined threshold parameter and $\gamma \in [0, 1)$. The ZOH receives the current data, promptly changes its store, and activates the controller if the ET condition in (8) is infringed. When $k > k_\wp$ and ET condition (8) is incorrect, the next triggering instant $k_{\wp+1}$ is

$$k_{\wp+1} = \inf\left\{k > k_\wp \left|\left\|\mathbf{e}_{k_\wp}(k)\right\|_1 > \gamma\|\mathbf{x}(k)\|_1\right.\right\}, \tag{9}$$

where $k_{\wp+1}$ is the $(\wp+1)^{th}$ release instant from the sensor end to the controller end.

Remark 3: The ETC mechanism is introduced in the network environment, and only the sampling state that exceeds the threshold in (8) will be sent to the controller. Compared with the periodic sampling mechanism, it can effectively reduce the network resource consumption and alleviate the congestion appearance. If one set $\gamma = 0$, then the ETC scheme (8) is simplified to the periodic time-triggered scheme.

Remark 4: For DPPFNC systems with time delay, the quadratic Lyapunov function will bring conservatism, and the linear co-determination Lyapunov function (LCLF) [37] is more suitable for stability analysis. Under the framework of

LCLF, an event-triggered condition in linear form is more appropriate. Meanwhile, the 1-norm event-triggered condition is more convenient to scale and estimate the state quantity. The 1-norm describes the sum of the absolute vector components, so it can preferably denote the number of biological populations, the liquid level in the reservoir vessel, the density of matter in physics, and other variables that remain non-negative values all the time. Unlike the results that consider the time delay in event-triggered conditions, the plant of our paper is the time delay DPPFNC systems.

D. IT2 Polynomial Fuzzy Event-Triggered Controller

An IT2 polynomial fuzzy event-triggered controller is developed based on the IPM concept under limited communication bandwidth with the ET condition (8). The structure of the j^{th} rule is as follows:

Rule j : IF $g_1(\mathbf{x}(k_\wp))$ is $\tilde{N}_1^j$ AND $\cdots$ AND $g_\Omega(\mathbf{x}(k_\wp))$ is $\tilde{N}_\Omega^j$ THEN $\quad \mathbf{u}(k_\wp) = \mathbf{G}_j\mathbf{x}(k_\wp)$, (10)

where $\mathbf{x}(k_\wp)$ is the state at the ET time and $k \in [k_\wp, k_{\wp+1})$ with $t \in \mathbb{N}$, and $k_0 = 0$. $\tilde{N}_\beta^j$ is the IT2 fuzzy set of premise variable $g_\beta(\mathbf{x}(k_\wp))$ under the j^{th} rule, $i \in \underline{p}$, $j \in \underline{c}, \beta \in \underline{\Omega}$; The event-triggered feedback gains are $\mathrm{G}_j \in \Re^{m\times n}$, and they must be found.

The next interval sets describe the firing strength under the jth rule:

$$M_j(\mathbf{x}(k_\wp)) \in \left[m_j^L(\mathbf{x}(k_\wp)), m_j^U(\mathbf{x}(k_\wp))\right], \qquad \forall j, \tag{11}$$

in which $m_j^L(\mathbf{x}(k_\wp)) = \prod_{\beta=1}^{\Omega} \underline{\mu}_{\tilde{N}_\beta^j}(g_\beta(\mathbf{x}(k_\wp)))$ represent the lower grades of membership, $m_j^U(\mathbf{x}(k_\wp)) = \prod_{\beta=1}^{\Omega} \bar{\mu}_{\tilde{N}_\beta^j}(g_\beta(\mathbf{x}(k_\wp)))$ represent the upper grades of membership. $\underline{\mu}_{\tilde{N}_\beta^j}(g_\beta(\mathbf{x}(k_\wp))) \geq 0$ represent the lower MFs, $\bar{\mu}_{\tilde{N}_\beta^j}(g_\beta(\mathbf{x}(k_\wp))) \geq 0$ represent the upper MFs. Furthermore, for all j, it exhibits the property that $0 \leq \underline{\mu}_{\tilde{N}_\beta^j}(g_\beta(\mathbf{x}(k_\wp))) \leq \bar{\mu}_{\tilde{N}_\beta^j}(g_\beta(\mathbf{x}(k_\wp))) \leq 1$, which brings about $0 \leq m_j^L(\mathbf{x}(k_\wp)) \leq m_j^U(\mathbf{x}(k_\wp)) \leq 1$.

An IT2 fuzzy ET controller is represented by:

$$\mathbf{u}(k_\wp) = \sum_{j=1}^{c} \tilde{m}_j(\mathbf{x}(k_\wp))\mathbf{G}_j\mathbf{x}(k_\wp), \tag{12}$$

in which

$$\tilde{m}_j(\mathbf{x}(k_\wp)) = \frac{\underline{\kappa}_j(\mathbf{x}(k_\wp))m_j^L(\mathbf{x}(k_\wp)) + \bar{\kappa}_j(\mathbf{x}(k_\wp))m_j^U(\mathbf{x}(k_\wp))}{\sum_{k=1}^{c}\Big(\underline{\kappa}_j(\mathbf{x}(k_\wp))m_k^L(\mathbf{x}(k_\wp)) + \bar{\kappa}_j(\mathbf{x}(k_\wp))m_k^U(\mathbf{x}(k_\wp))\Big)}, \tag{13}$$

$$\sum_{j=1}^{c} \tilde{m}_j(\mathbf{x}(k_\wp)) = 1, \tilde{m}_j(\mathbf{x}(k_\wp)) \geq 0, \qquad \forall j, \tag{14}$$

$\tilde{m}_j(\mathbf{x}(k_\wp))$ are the grades of the embedded MFs containing only $\mathbf{x}(k)$, consistent with the premise variable $g_\beta(\mathbf{x}(k_\wp))$, independent of the term $\mathbf{x}(k-\tau)$. (13) is the type reduction. $\underline{\kappa}_j(\mathbf{x}(k_\wp))$ and $\bar{\kappa}_j(\mathbf{x}(k_\wp))$ are predefined functions, for all j, have properties of $0 \leq \underline{\kappa}_j(\mathbf{x}(k_\wp)) \leq \bar{\kappa}_j(\mathbf{x}(k_\wp)) \leq 1$, $\underline{\kappa}_j(\mathbf{x}(k_\wp)) + \bar{\kappa}_j(\mathbf{x}(k_\wp))= 1$.

Remark 5: Since the event-triggered fuzzy controller can only observe triggering state after triggering action, it's not difficult to find that the premise variables of different time scales are employed in the polynomial fuzzy model and the event-triggered controller. This assumption is also widely used in the existing studies on the FMB NCSs with the ETC mechanism [20], [21]. Meanwhile, the existence of the ETC mechanism leads to asynchronous premises, and the PDC technology is no longer applicable.

III. Event-Triggered Stability Abalysis

The closed-loop system with the discrete-time IT2 polynomial fuzzy model (4), the event-triggered controllers (12) under 1-norm event-triggered condition (8) is described by:

$$\mathbf{x}(k+1) = \sum_{i=1}^{p}\sum_{j=1}^{c} \tilde{w}_i(\mathbf{x}(k))\tilde{m}_j(\mathbf{x}(k_\wp))\Big(\mathbf{A}_i(\mathbf{x}(k))\mathbf{x}(k) + \mathbf{A}_{\tau i}(\mathbf{x}(k))\mathbf{x}(k-\tau) + \mathbf{B}_i(\mathbf{x}(k))\mathbf{G}_j\mathbf{x}(k_\wp)\Big). \tag{15}$$

A. Basic Stability Analysis for Time Delay Event-Trigger-Based DPPFNC Systems

For $x(k_0) \geq 0$, we can obtain from event-triggered condition (8) that $\left\|\mathbf{e}_{k_\wp}(k)\right\|_1 \leq \gamma\mathbf{1}_n^T\mathbf{x}(k)$, which leads to

$$-\gamma\mathbf{1}_{n\times n}\mathbf{x}(k) \leq \mathbf{e}_{k_\wp}(k) \leq \gamma\mathbf{1}_{n\times n}\mathbf{x}(k). \tag{16}$$

From (7) and (15), it is easy to get

$$\begin{aligned}\mathbf{x}(k+1) &= \sum_{j=1}^{c}\sum_{i=1}^{p} \tilde{w}_i(\mathbf{x}(k))\tilde{m}_j(\mathbf{x}(k_\wp))\Big(\mathbf{A}_i(\mathbf{x}(k))\mathbf{x}(k) + \mathbf{A}_{\tau i}(\mathbf{x}(k))\mathbf{x}(k-\tau) + \mathbf{B}_i(\mathbf{x}(k))\mathbf{G}_j\Big(\mathbf{x}(k)+\mathbf{e}_{k_\wp}(k)\Big)\Big)\\ &= \sum_{j=1}^{c}\sum_{i=1}^{p} \tilde{w}_i(\mathbf{x}(k))\tilde{m}_j(\mathbf{x}(k_\wp))\Big(\Big(\mathbf{A}_i(\mathbf{x}(k)) + \mathbf{B}_i(\mathbf{x}(k))\mathbf{G}_j\Big)\mathbf{x}(k) + \mathbf{B}_i(\mathbf{x}(k))\mathbf{G}_j\mathbf{e}_{k_\wp}(k) + \mathbf{A}_{\tau i}(\mathbf{x}(k))\mathbf{x}(k-\tau)\Big).\end{aligned} \tag{17}$$

where the ETC gain $\mathbf{G}_j$ is designed as $\mathbf{G}_j = \mathbf{G}_j^+ + \mathbf{G}_j^-$, $\mathbf{G}_j^+ \succ 0$ and $\mathbf{G}_j^- \prec 0$. Since $\mathbf{B}_i(\mathbf{x}(k)) \geq 0$, the following inequations are obtained:

$$\begin{aligned}-\gamma\mathbf{B}_i(\mathbf{x}(k))\mathbf{G}_j^+\mathbf{1}_{n\times n}\mathbf{x}(k) &\leq \mathbf{B}_i(\mathbf{x}(k))\mathbf{G}_j^+\mathbf{e}_{k_\wp}(k)\\ &\leq \gamma\mathbf{B}_i(\mathbf{x}(k))\mathbf{G}_j^+\mathbf{1}_{n\times n}\mathbf{x}(k).\end{aligned} \tag{18}$$

$$\begin{aligned}\gamma\mathbf{B}_i(\mathbf{x}(k))\mathbf{G}_j^-\mathbf{1}_{n\times n}\mathbf{x}(k) &\leq \mathbf{B}_i(\mathbf{x}(k))\mathbf{G}_j^-\mathbf{e}_{k_\wp}(k)\\ &\leq -\gamma\mathbf{B}_i(\mathbf{x}(k))\mathbf{G}_j^-\mathbf{1}_{n\times n}\mathbf{x}(k).\end{aligned} \tag{19}$$

Together with (17) follows that

$$\mathbf{x}(k+1) \geq \sum_{i=1}^{p}\sum_{j=1}^{c} \tilde{w}_i(\mathbf{x}(k))\tilde{m}_j(\mathbf{x}(k_\wp)) \times \Big(\mathbf{A}_i(\mathbf{x}(k))\mathbf{x}(k) + \mathbf{B}_i(\mathbf{x}(k))\mathbf{G}_j^+\mathbf{x}(k) + \mathbf{B}_i(\mathbf{x}(k))\mathbf{G}_j^-\mathbf{x}(k)$$

$$
\begin{aligned}
&- \gamma\mathbf{B}_i(\mathbf{x}(k))\mathbf{G}_j^+\mathbf{1}_{n\times n}\mathbf{x}(k) + \gamma\mathbf{B}_i(\mathbf{x}(k))\mathbf{G}_j^-\mathbf{1}_{n\times n}\mathbf{x}(k) \\
&+ \mathbf{A}_{\tau i}(\mathbf{x}(k))\mathbf{x}(k-\tau)\Big) \\
&= \sum_{i=1}^{p}\sum_{j=1}^{c}\tilde{w}_i(\mathbf{x}(k))\tilde{m}_j(\mathbf{x}(k_\wp))\bigg(\Big(\mathbf{A}_i(\mathbf{x}(k)) + \mathbf{B}_i(\mathbf{x}(k))\mathbf{G}_j^+\mathbf{\Theta} \\
&+ \mathbf{B}_i(\mathbf{x}(k))\mathbf{G}_j^-\mathbf{\Phi}\Big)\mathbf{x}(k) + \mathbf{A}_{\tau i}(\mathbf{x}(k))\mathbf{x}(k-\tau)\bigg), \qquad (20)
\end{aligned}
$$

where $\mathbf{\Theta} \in \Re^{n\times n}$ and $\mathbf{\Phi} \in \Re^{n\times n}$ are matrices corresponding to the ETC mechanism threshold γ. And, $\mathbf{\Theta} = I - \gamma\mathbf{1}_{n\times n}$, $\mathbf{\Phi} = I + \gamma\mathbf{1}_{n\times n}$, $\mathbf{T}_{ij}(\mathbf{x}(k)) = \mathbf{A}_i(\mathbf{x}(k)) + \mathbf{B}_i(\mathbf{x}(k))\mathbf{G}_j^+\mathbf{\Theta} + \mathbf{B}_i(\mathbf{x}(k))\mathbf{G}_j^-\mathbf{\Phi}$, for $i \in \underline{p}, j \in \underline{c}$.

Noting the fact $x(k_0) \geq 0$, $x(k_0+1) \geq 0$ holds if $\mathbf{T}_{ij}(x(k_0)) \geq 0$ for all i and j. Otherwise, $\mathbf{A}_{\tau i}(\mathbf{x}(k)) > 0$. It is simple to demonstrate that $\mathbf{x}(k) \geq 0$ for initial states $x(k_0) \geq 0$ and $\mathbf{T}_{ij}(x(k)) \geq 0$ using recursive derivation. As a result, the system's (15) positive property is established.

Next, LCLF, which is more suitable for positive systems, is considered to obtain the stability criteria related to the time delay DPPFNC system (15) with unique positive constraints.

$$
\mathbf{V}(\mathbf{x}(k)) = \boldsymbol{\lambda}^T\mathbf{x}(k) + \sum_{m=1}^{p}\sum_{s=k-\tau}^{k-1}\Big(\boldsymbol{\lambda}^T\mathbf{A}_{\tau m}(\mathbf{x}(s))\mathbf{x}(s)\Big), \qquad (21)
$$

in which $\boldsymbol{\lambda} = [\lambda_1, \lambda_2, ..., \lambda_n]^T \succ 0$ is a constant vector to be determined.

According to Lyapunov stability theory, when $\mathbf{V}(\mathbf{x}(k)) > 0$, $\Delta\mathbf{V}(\mathbf{x}(k)) < 0$ for all $x \neq 0$, the time delay DPPFNC system is asymptotically stable. Then,

$$
\begin{aligned}
&\Delta\mathbf{V}(\mathbf{x}(k)) = \mathbf{V}(\mathbf{x}(k+1)) - \mathbf{V}(\mathbf{x}(k)) \\
&\leq \boldsymbol{\lambda}^T\sum_{i=1}^{p}\sum_{j=1}^{c}\tilde{w}_i(\mathbf{x}(k))\tilde{m}_j(\mathbf{x}(k_\wp))\bigg(\Big(\mathbf{A}_i(\mathbf{x}(k)) + \mathbf{B}_i(\mathbf{x}(k))\mathbf{G}_j \\
&- \mathbf{I}\Big)\mathbf{x}(k) + \mathbf{B}_i(\mathbf{x}(k))\mathbf{G}_j\mathbf{e}_{k_\wp}(k)\bigg) + \sum_{i=1}^{p}(\boldsymbol{\lambda}^T\mathbf{A}_{\tau i}(\mathbf{x}(k))\mathbf{x}(k-\tau)) \\
&+ \sum_{m=1}^{p}\big(\boldsymbol{\lambda}^T\mathbf{A}_{\tau m}(\mathbf{x}(k))\mathbf{x}(k)\big) - \sum_{m=1}^{p}\big(\boldsymbol{\lambda}^T\mathbf{A}_{\tau m}(\mathbf{x}(k))\mathbf{x}(k-\tau)\big) \\
&\leq \boldsymbol{\lambda}^T\sum_{i=1}^{p}\sum_{j=1}^{c}\tilde{w}_i(\mathbf{x}(k))\tilde{m}_j(\mathbf{x}(k_\wp))\bigg(\Big(\mathbf{A}_i(\mathbf{x}(k)) + \mathbf{B}_i(\mathbf{x}(k))\mathbf{G}_j^+ \\
&+ \mathbf{B}_i(\mathbf{x}(k))\mathbf{G}_j^- + \gamma\mathbf{B}_i(\mathbf{x}(k))\mathbf{G}_j^+\mathbf{1}_{n\times n} - \gamma\mathbf{B}_i(\mathbf{x}(k))\mathbf{G}_j^-\mathbf{1}_{n\times n} \\
&- \mathbf{I}\Big)\mathbf{x}(k)\bigg) + \sum_{m=1}^{p}\boldsymbol{\lambda}^T\mathbf{A}_{\tau m}(\mathbf{x}(k))\mathbf{x}(k) \\
&= \sum_{i=1}^{p}\sum_{j=1}^{c}\tilde{w}_i(\mathbf{x}(k))\tilde{m}_j(\mathbf{x}(k_\wp))\bigg(\boldsymbol{\lambda}^T\Big(\mathbf{A}_i(\mathbf{x}(k)) - \mathbf{I}\Big) \\
&+ \boldsymbol{\lambda}^T\mathbf{B}_i(\mathbf{x}(k))\mathbf{G}_j^+\mathbf{\Phi} + \boldsymbol{\lambda}^T\mathbf{B}_i(\mathbf{x}(k))\mathbf{G}_j^-\mathbf{\Theta} \\
&+ \sum_{m=1}^{p}\boldsymbol{\lambda}^T\mathbf{A}_{\tau m}(\mathbf{x}(k))\bigg)\mathbf{x}(k), \qquad (22)
\end{aligned}
$$

where $\mathbf{Q}_{ij}(\mathbf{x}(k)) = \boldsymbol{\lambda}^T\Big(\mathbf{A}_i(\mathbf{x}(k)) + \sum_{m=1}^{p}\mathbf{A}_{\tau m}(\mathbf{x}(k)) - \mathbf{I}\Big) + \boldsymbol{\lambda}^T\mathbf{B}_i(\mathbf{x}(k))\mathbf{G}_j^+\mathbf{\Phi} + \boldsymbol{\lambda}^T\mathbf{B}_i(\mathbf{x}(k))\mathbf{G}_j^-\mathbf{\Theta}$ with $i \in \underline{p}; j \in \underline{c}$; $\mathbf{\Theta} = \mathbf{I} - \gamma\mathbf{1}_{n\times n}$, $\mathbf{\Phi} = \mathbf{I} + \gamma\mathbf{1}_{n\times n}$. $\Delta\mathbf{V}(k) < 0$ holds if $\mathbf{Q}_{ij}(\mathbf{x}(k)) \prec 0$. However, $\lambda^T\mathbf{B}_i(\mathbf{x}(k))\mathbf{G}_j^+\mathbf{\Phi}$ and $\lambda^T\mathbf{B}_i(\mathbf{x}(k))\mathbf{G}_j^-\mathbf{\Theta}$ are non-convex terms of $\mathbf{Q}_{ij}(\mathbf{x}(k))$, which increases challenge in solving stability conditions in the SOS-TOOLS.

To solve this problem, we denote $\mathbf{G}_j^+ = \mathbf{I}_m\mathbf{g}_j^+$ and $\mathbf{G}_j^- = \mathbf{I}_m\mathbf{g}_j^-$, the following equation is obtained:

$$
\boldsymbol{\lambda}^T\mathbf{B}_i(\mathbf{x}(k))\mathbf{I}_m\mathbf{g}_j^+ = \mathbf{M}_{ij}^+(\mathbf{x}(k)), \qquad (23)
$$

$$
\boldsymbol{\lambda}^T\mathbf{B}_i(\mathbf{x}(k))\mathbf{I}_m\mathbf{g}_j^- = \mathbf{M}_{ij}^-(\mathbf{x}(k)). \qquad (24)
$$

After the above series of transformations, $\mathbf{G}_j^+$ and $\mathbf{G}_j^-$ can be obtained.

$$
\mathbf{G}_j^{\pm} = \frac{\mathbf{I}_m\mathbf{M}_{ij}^{\pm}(\mathbf{x}(k))}{\boldsymbol{\lambda}^T\mathbf{B}_i(\mathbf{x}(k))\mathbf{I}_m}, \qquad (25)
$$

$\mathbf{M}_{ij}^{\pm}(\mathbf{x}(k)) \in \Re^{1\times n}$ is polynomial vectors to be determined. And $\mathbf{I}_m = \Big[\underbrace{1, 1, ..., 1}_{m}\Big]^T$. From $\mathbf{B}_i(\mathbf{x}(k)) \succ 0$ and $\boldsymbol{\lambda} = [\lambda_1, \lambda_2, ..., \lambda_n]^T \succ 0$, hence, the denominator $\boldsymbol{\lambda}^T\mathbf{B}_i(\mathbf{x}(k))\mathbf{I}_m$ is a positive scalar. The feedback gain satisfies $\mathbf{G}_j = \mathbf{G}_j^+ + \mathbf{G}_j^-$.

To solve the non-convex term in the stability analysis, taking (23) and (24) into $\mathbf{Q}_{ij}(x(k))$, we can get

$$
\begin{aligned}
\mathbf{Q}_{ij}(\mathbf{x}(k)) =& \boldsymbol{\lambda}^T\Big(\mathbf{A}_i(\mathbf{x}(k)) + \sum_{m=1}^{p}\mathbf{A}_{\tau m}(\mathbf{x}(k)) - \mathbf{I}\Big) \\
&+ \mathbf{M}_{ij}^+(\mathbf{x}(k))\mathbf{\Phi} + \mathbf{M}_{ij}^-(\mathbf{x}(k))\mathbf{\Theta}. \qquad (26)
\end{aligned}
$$

From (22), when $\mathbf{Q}_{ij} \prec 0$, $\Delta\mathbf{V}(\mathbf{x}(k)) < 0$. In addition, based on (25), the positive condition $\mathbf{T}_{ij}(\mathbf{x}(k))$ is derived:

$$
\begin{aligned}
\mathbf{T}_{ij}(\mathbf{x}(k)) =& \mathbf{A}_i(\mathbf{x}) + \mathbf{B}_i(\mathbf{x})\mathbf{I}_m\frac{\mathbf{M}_{ij}^+(\mathbf{x})}{\boldsymbol{\lambda}^T\mathbf{B}_i(\mathbf{x})\mathbf{I}_m}\mathbf{\Theta} \\
&+ \mathbf{B}_i(\mathbf{x})\mathbf{I}_m\frac{\mathbf{M}_{ij}^-(\mathbf{x})}{\boldsymbol{\lambda}^T\mathbf{B}_i(\mathbf{x})\mathbf{I}_m}\mathbf{\Phi} \geq 0. \qquad (27)
\end{aligned}
$$

Since $\boldsymbol{\lambda}^T\mathbf{B}_i(\mathbf{x})\mathbf{I}_m$ mentioned above is a positive scalar, if $\boldsymbol{\lambda}^T\mathbf{B}_i(\mathbf{x})\mathbf{I}_m\mathbf{A}_i(\mathbf{x}) + \mathbf{B}_i(\mathbf{x})\mathbf{I}_m\mathbf{M}_{ij}^+(\mathbf{x})\mathbf{\Theta} + \mathbf{B}_i(\mathbf{x})\mathbf{I}_m\mathbf{M}_{ij}^-(\mathbf{x})\mathbf{\Phi} \geq 0$ satisfies $\mathbf{T}_{ij}(\mathbf{x}(k)) \succeq 0$. Therefore, the convex positive conditions for the system (15) can be obtained.

Remark 6: The matrix decomposition technique is employed to parameterize the gain matrix as a combination of non-positive and non-negative components, as shown by $\mathbf{G}_j = \mathbf{G}_j^+ + \mathbf{G}_j^-$. Through (18) and (19), the error term $e_{k_\wp}(k)$ can easily be converted to the term $x(k)$ and the positivity and stability criteria can be easily derived.

The following theorem states the fundamental positivity and stability conditions of SOS form that ensure the positivity and stability of DPPFNC system (15).

Theorem 1: For time delay DPPFNC system (15) under the ETC scheme (8), if there exist prescribed positive scalars $0 < \gamma \leq 1$, vectors $\boldsymbol{\lambda}$, $\boldsymbol{\theta}_s$, $\boldsymbol{\phi}_s \in \Re^n$ make the following SOS conditions hold with $i \in \underline{p}$, $j \in \underline{c}$ and $s \in \underline{n}$:

$$
\lambda_s - \varepsilon_1 \text{ is SOS}; s \in \underline{n}, \qquad (28)
$$

$$a_{fs}^{\tau i}(\mathbf{x}(k)) \text{ is SOS}; i \in \underline{p}, f = s \in \underline{n}, \tag{29}$$

$$m_s^{ij+}(\mathbf{x}(k)) - \varepsilon_2(\mathbf{x}(k)) \text{ is SOS}; s \in \underline{n}, \tag{30}$$

$$-(m_s^{ij-}(\mathbf{x}(k)) + \varepsilon_2(\mathbf{x}(k))) \text{ is SOS}; s \in \underline{n}, \tag{31}$$

$$\boldsymbol{\lambda}^T \mathbf{B}_i(\mathbf{x}(k))\mathbf{I}_m a_{fs}^i(\mathbf{x}(k)) + \mathbf{b}_f^i(\mathbf{x}(k))\mathbf{I}_m \mathbf{M}_{ij}^+(\mathbf{x}(k))\boldsymbol{\theta}_s + \mathbf{b}_f^i(\mathbf{x}(k))\mathbf{I}_m \mathbf{M}_{ij}^-(\mathbf{x}(k))\boldsymbol{\phi}_s \text{ is SOS}; i \in \underline{p}, j \in \underline{c}, f, s \in \underline{n}, \tag{32}$$

$$-\Big(q_s^{ij}(\mathbf{x}(k)) + \varepsilon_2(\mathbf{x}(k))\Big) \text{ is SOS}; i \in \underline{p}, j \in \underline{c}, f, s \in \underline{n}, \tag{33}$$

in which $\varepsilon_1 > 0$ and $\varepsilon_2(\mathbf{x}(k)) > 0$ for $\mathbf{x}(k) \neq 0$ are predefined scalar and predefined scalar polynomial, respectively. $\mathbf{A}_i(\mathbf{x}(k)) = (a_{fs}^i(\mathbf{x}(k)))$, $\mathbf{A}_{\tau i}(\mathbf{x}(k-\tau)) = (a_{fs}^{\tau i}(\mathbf{x}(k)))$ and $\mathbf{B}_i(\mathbf{x}(k)) = [\mathbf{b}_1^{iT}(\mathbf{x}(k)), \mathbf{b}_2^{iT}(\mathbf{x}(k)), ..., \mathbf{b}_n^{iT}(\mathbf{x}(k))]^T$, $\forall i \in \underline{p}$, $f, s \in \underline{n}$. $\boldsymbol{\Theta}= [\boldsymbol{\theta}_1, \boldsymbol{\theta}_2,...,\boldsymbol{\theta}_n]$, $\boldsymbol{\Phi}= [\boldsymbol{\phi}_1, \boldsymbol{\phi}_2,...,\boldsymbol{\phi}_n]$. $\mathbf{Q}_{ij}(\mathbf{x}(k)) = [q_1^{ij}(\mathbf{x}(k)), q_2^{ij}(\mathbf{x}(k)), ..., q_n^{ij}(\mathbf{x}(k))]^T$, $\forall i \in \underline{p}$, $j \in \underline{c}$; (25) shows the event-triggered feedback gains.

Remark 7: Under IPM technology, we can derive the basic positivity and stability conditions in SOS form of an event-triggered-based DPPFNC system with time delay from Theorem 1. Still, the stability criteria in Theorem 1 is MFs-independent. Besides, due to the limitation of the convex optimization toolbox, it can only recognize specific polynomial form MFs. It is necessary to convert the known MFs into polynomial forms that the toolbox can recognize.

B. Genetic Algorithm Membership Function

For simplicity, the following equation brings in information about IT2-MFs by reconstructing the original IT2-MFs [38] as:

$$\begin{aligned}\tilde{h}_{ij}(\mathbf{x}(k), \mathbf{x}(k_\wp)) &\equiv \tilde{w}_i(\mathbf{x}(k))\tilde{m}_j(\mathbf{x}(k_\wp)) \\ &= \underline{\beta}_{ij}(\mathbf{x}(k), \mathbf{x}(k_\wp))\underline{h}_{ij}(\mathbf{x}(k), \mathbf{x}(k_\wp)) \\ &\quad + \bar{\beta}_{ij}(\mathbf{x}(k), \mathbf{x}(k_\wp))\bar{h}_{ij}(\mathbf{x}(k), \mathbf{x}(k_\wp)),\end{aligned} \tag{34}$$

where $\sum_{i=1}^{p}\sum_{j=1}^{c} \tilde{h}_{ij}(\mathbf{x}(k), \mathbf{x}(k_\wp)) = 1$, $\underline{\beta}_{ij}(\mathbf{x}(k), \mathbf{x}(k_\wp))$ and $\bar{\beta}_{ij}(\mathbf{x}(k), \mathbf{x}(k_\wp))$ are nonlinear functions that not necessary to be known but exist, satisfying $\underline{\beta}_{ij}(\mathbf{x}(k), \mathbf{x}(k_\wp)) + \bar{\beta}_{ij}(\mathbf{x}(k), \mathbf{x}(k_\wp))$=1, $\forall i \in \underline{p}$, $\forall j \in \underline{c}$.

Remark 8: The IT2 MF $\tilde{h}_{ij}(\mathbf{x}(k), \mathbf{x}(k_\wp))$ is reconfigurable into a linear combination of $\underline{h}_{ij}(\mathbf{x}(k), \mathbf{x}(k_\wp))$ and $\bar{h}_{ij}(\mathbf{x}(k), \mathbf{x}(k_\wp))$.

Since the polynomial approximation is performed in each operating subdomain, the L linked run subdomains $\boldsymbol{\Psi}_l$, $l \in \underline{L}$, make up the entire run domain (denoted $\boldsymbol{\Psi}$), so $\boldsymbol{\Psi} = \cup_{l=1}^{L}\psi_l$. At time k, denote $\hat{\underline{h}}_{ijl}(\alpha_{ij}, \mathbf{x}(k))$ to approximate $\underline{h}_{ij}(\mathbf{x}(k), \mathbf{x}(k_\wp))$ in each subdomain $\boldsymbol{\Psi}_l$. Next, define a finite-dimensional linear space $\aleph_n$ of no more than n times, and its element is

$$\hat{\underline{h}}_{ijl}(\alpha_{ij}, \mathbf{x}(k)) = a_{0ij} + \sum_{g=1}^{n} a_{gij}\chi_g(\mathbf{x}(k)), \tag{35}$$

where $\{1, \chi_1(\mathbf{x}(k)), \chi_2(\mathbf{x}(k)), ..., \chi_n(\mathbf{x}(k))\}$ is a linearly independent set of basis about $\aleph_n$, so $\aleph_n = span\{1, \chi_1(\mathbf{x}(k)), \chi_2(\mathbf{x}(k)), ..., \chi_n(\mathbf{x}(k))\}$, $\aleph_n$ is $n+1$ dimension; $\alpha_{ij} = (a_{0ij}, a_{1ij}, ..., a_{nij})$ is the coordinate vector of $\hat{\underline{h}}_{ijl}(\alpha_{ij}, \mathbf{x}(k))$.

Remark 9: Common polynomial interpolation approximation methods, such as Taylor approximation method use the approximation order to judge the approximation quality. But the existence of the Runge phenomenon shows that even if the approximation order is very high, the overall approximation error cannot be reduced. Therefore, starting from the theory of optimum uniform approximation, the uniform norm is introduced into space from the perspective of overall approximation, and approximation quality is controlled by the uniform norm. The following Weierstrass approximation theory proves the optimum uniform approximation polynomial exists.

For continuous function $f(x) \in C[a, b]$, any element of $f(x)$ can be approximated by the finite-dimensional polynomial $p(x) \in H_n$, making the error $\mathbf{E}_n(f) < \varepsilon$ ($\varepsilon > 0$ is any given). This is known as Weierstrass approximation theory [39]:

Lemma 2: Suppose that $f(x) \in C[a, b]$, there exists a polynomial $p(x)$, given any $\varepsilon > 0$ that satisfies

$$\|f(x) - p(x)\|_\infty < \varepsilon, \forall x \in [a, b].$$

The existence of $p(x)$ can be proved by the Weierstrass approximation theorem according to lemma 2 above, combined with the theory of optimal uniform approximation to find the minimum deviation and its corresponding optimal uniform approximation polynomial. The infinite norm of the deviation between $\underline{h}_{ijl}(\mathbf{x}(k), \mathbf{x}(k_\wp))$ and $\hat{\underline{h}}_{ijl}(\alpha_{ij}, \mathbf{x}(k))$ on $\pounds$ is

$$\begin{aligned}&\Big\|\Delta\Big(\underline{h}_{ijl}(\alpha_{ij}, \mathbf{x}(k))\Big)\Big\|_\infty \\ &= \Big\|\underline{h}_{ijl}(\mathbf{x}(k), \mathbf{x}(k_\wp)) - \hat{\underline{h}}_{ijl}(\alpha_{ij}, \mathbf{x}(k))\Big\|_\infty \\ &= \max_{\mathbf{x}\in\pounds}\Big|\underline{h}_{ijl}(\mathbf{x}(k), \mathbf{x}(k_\wp)) - \hat{\underline{h}}_{ijl}(\alpha_{ij}, \mathbf{x}(k))\Big|.\end{aligned} \tag{36}$$

Remark 10: $\pounds$ is a predefined compact subset of Banach space, $\pounds = \{(x_1, ..., x_n)\,|-\infty \prec a_i \leq x_i \leq b_i \prec \infty, i = 1, ..., n\}$, x_i satisfy $x_i \in [a_i, b_i]$.

Obviously, $\Big\|\Delta\Big(\underline{h}_{ijl}(\alpha_{ij}, \mathbf{x}(k))\Big)\Big\|_\infty \geq 0$, the lower bound of the set $\{\Big\|\Delta\Big(\underline{h}_{ijl}(\alpha_{ij}, \mathbf{x}(k))\Big)\Big\|_\infty\}$ denoted as:

$$\begin{aligned}&\mathbf{E}\Big(\underline{h}_{ijl}(\alpha_{ij}, \mathbf{x}(k))\Big) \\ &= \inf_{\hat{\underline{h}}_{ijl}(\alpha_{ij}, \mathbf{x}(k))\in\aleph_n}\{\Big\|\Delta\Big(\underline{h}_{ijl}(\alpha_{ij}, \mathbf{x}(k))\Big)\Big\|_\infty\} \\ &= \inf_{\hat{\underline{h}}_{ijl}(\alpha_{ij}, \mathbf{x}(k))\in\aleph_n}\max_{\mathbf{x}\in\pounds}\Big|\underline{h}_{ijl}(\mathbf{x}(k), \mathbf{x}(k_\wp)) - \hat{\underline{h}}_{ijl}(\alpha_{ij}, \mathbf{x}(k))\Big|,\end{aligned} \tag{37}$$

$\mathbf{E}\Big(\underline{h}_{ijl}(\alpha_{ij}, \mathbf{x}(k))\Big)$, called the minimum deviation of $\underline{h}_{ijl}(\mathbf{x}(k), \mathbf{x}(k_\wp))$ on $\pounds$. If there is $\hat{\underline{h}}_{ijl}^*\left(\alpha_{ij}^*, \mathbf{x}(k)\right) \in \aleph_n$ that satisfies the following equation:

$$\Big\|\Delta\Big(\underline{h}_{ijl}^*\left(\alpha_{ij}^*, \mathbf{x}(k)\right)\Big)\Big\|_\infty$$

$$= \max_{\mathbf{x}\in\pounds} \left| \underline{h}_{ijl}(\mathbf{x}(k), \mathbf{x}(k_\wp)) - \hat{\underline{h}}^*_{ijl}\left(\alpha^*_{ij}, \mathbf{x}(k)\right) \right|$$
$$= \inf_{\hat{\underline{h}}_{ijl}(\alpha_{ij},\mathbf{x}(k))\in\aleph_n} \max_{\mathbf{x}\in\pounds} \left| \underline{h}_{ijl}(\mathbf{x}(k), \mathbf{x}(k_\wp)) - \hat{\underline{h}}_{ijl}(\alpha_{ij}, \mathbf{x}(k)) \right|$$
$$= \mathbf{E}(\underline{h}_{ijl}(\alpha_{ij}, \mathbf{x}(k))), \tag{38}$$

where $\hat{\underline{h}}^*_{ijl}\left(\alpha^*_{ij}, \mathbf{x}(k)\right)$ is the optimum uniform approximation polynomials of $\underline{h}_{ijl}(\mathbf{x}(k), \mathbf{x}(k_\wp))$ on $\pounds$. The symbolic function $\left\|\Delta(\underline{h}^*_{ijl}\left(\alpha^*_{ij}, \mathbf{x}(k)\right))\right\|_\infty$ derived from the minimal problem is called the optimum uniform norm (the minimum of the maximum approximation error).

The original lower MFs is reexpressed as:

$$\underline{h}_{ijl}(\mathbf{x}(k), \mathbf{x}(k_\wp)) = \varsigma_l(\mathbf{x})\Big(\hat{\underline{h}}^*_{ijl}\left(\alpha^*_{ij}, \mathbf{x}(k)\right) + \Delta\Big(\underline{h}^*_{ijl}\left(\alpha^*_{ij}, \mathbf{x}(k)\right)\Big)\Big), \tag{39}$$

$\varsigma_l(\mathbf{x}) = 1$ if $\mathbf{x} \in \mathbf{\Psi}_l$, $l \in \underline{L}$; otherwise, $\varsigma_l(\mathbf{x}) = 0$. From (35), the optimum uniform approximation functions are

$$\hat{\underline{h}}^*_{ijl}(\alpha^*_{ij}, \mathbf{x}(k)) = a^*_{0ij} + \sum_{g=1}^{n} a^*_{gij}\chi_g(\mathbf{x}(k)), \tag{40}$$

where $\alpha^*_{ij} = \left(a^*_{0ij}, a^*_{1ij}, ..., a^*_{nij}\right)$ is the coordinate vector of $\hat{\underline{h}}^*_{ijl}(\alpha_{ij}, \mathbf{x}(k))$.

In this paper, each piecewise approximation polynomial $\hat{\underline{h}}_{ijl}\left(\alpha_{ij}, \mathbf{x}(k)\right)$ is optimized by GA individually, $\forall i \in \underline{p}, j \in \underline{c}, l \in \underline{L}$. The GA for solving the n^{th} degree optimum uniform approximation polynomial $\hat{\underline{h}}^*_{ijl}\left(\alpha^*_{ij}, \mathbf{x}(k)\right)$ and the minimum approximation error $\left\|\Delta(\underline{h}^*_{ijl}\left(\alpha^*_{ij}, \mathbf{x}(k)\right))\right\|_\infty$ is described as follows:

Step 1 (Chromosome representation and population initialisation) :

To simulate the biological evolution process, the optimization variable of the target problem should be expressed as the individual chromosome string structure. Each individual chromosome string structure a_{gij} is randomly generated as a binary string of length s from the genetic space, for example $a_{gij} = d_1 d_2 \ldots d_s$, $d_s \in \{0, 1\}$; so each individual in the population can be represented as $\alpha_{ij} = (a_{0ij}, a_{1ij}, ..., a_{nij}) = d_1 d_2 \ldots d_{n\times s}$. The population $P^{(1)}_{ij} \in \Re^{N\times(n\times s)}$ of N individuals is denoted as follows:

$$P^{(1)}_{ij} = \begin{bmatrix} \alpha^{(1,1)}_{ij} \\ \alpha^{(1,2)}_{ij} \\ \vdots \\ \alpha^{(1,N)}_{ij} \end{bmatrix} = \begin{bmatrix} a^{(1,1)}_{0ij} & a^{(1,1)}_{1ij} & \cdots & a^{(1,1)}_{nij} \\ a^{(1,2)}_{0ij} & a^{(1,2)}_{1ij} & \cdots & a^{(1,2)}_{nij} \\ \vdots & \vdots & \ddots & \vdots \\ a^{(1,N)}_{0ij} & a^{(1,N)}_{1ij} & \cdots & a^{(1,N)}_{nij} \end{bmatrix}.$$

Step 2 (Fitness calculation) :

Fitness is the basis for evaluating the pros and cons of an individual, and it will directly affect the reproduction and survival probability of an individual. To obtain the minimum maximum absolute approximation error (optimum uniform norm) and the optimum uniform approximation polynomial, the maximum absolute approximation error is used as the fitness function to evaluate the merits of N individuals $\alpha^{(t,n)}_{ij}$ in population $P^{(t)}_{ij}$. Combining this problem, find N elements in the array $\left[x^{(1,1)}_{1\max}, x^{(1,2)}_{1\max}, ..., x^{(1,N)}_{1\max}\right]^T$ within the range of x_1 that maximizes the fitness functions of each individual element in the array $\left[\left|\underline{h}_{ijl}(x_1) - \hat{\underline{h}}^{(1,1)}_{ijl}(\alpha^{(1,1)}_{ij}, x_1)\right|, \left|\underline{h}_{ijl}(x_1) - \hat{\underline{h}}^{(1,2)}_{ijl}(\alpha^{(1,2)}_{ij}, x_1)\right|\right.$ ..., $\left.\left|\underline{h}_{ijl}(x_1) - \hat{\underline{h}}^{(1,N)}_{ijl}(\alpha^{(1,N)}_{ij}, x_1)\right|\right]^T$, respectively.

Step 3 (Genetic operation) :

Genetic algorithm realizes the biological and population evolution processes through three basic operators: selection, crossover and mutation.

A fitness proportionate roulette wheel selection policy [40] is implemented for the selection process. If the corresponding fitness of individual k is $f^{(1,k)}_{ijl} = \left|\underline{h}_{ijl}(x^{(1,k)}_{1\max}) - \hat{\underline{h}}^{(1,k)}_{ijl}(\alpha^{(1,k)}_{ij}, x^{(1,k)}_{1\max})\right|$, then its selection probabilities within a population is $p^{(1,k)}_{ijl} = \left(1\Big/f^{(1,k)}_{ijl}\right)\Big/\sum_{i=1}^{N}\left(1\Big/f^{(1,i)}_{ijl}\right)$. In roulette wheel selection, individuals with smaller fitness have higher selection probabilities and are more likely to be selected for reproduction. Then, the single-point crossover operators are used to realize chromosome recombination and generate new individuals, ensuring the established evolutionary direction and generating species diversity. Following crossover each offspring undergoes mutation. This paper adopts a simple mutation operator to compensate for the lack of diversity.

Step 4 (Loop and termination operations) :

Record the optimal individuals in the current population after Step3 is completed, when the genetic algebra satisfies $T < 100$, the next generation evolution process is carried out and repeats Step 2 to Step 3. When the genetic algebra satisfies $T = 100$, the current approximation error is judged to be within the given range, such as $\mathbf{E}\Big(\underline{h}_{ijl}(\alpha_{ij}, \mathbf{x}(k))\Big) < 10^{-3}$. Finally, the optimal uniform approximation polynomial can be found.

C. IT2-MFD Stability Analysis for Time Delay Event-Trigger-Based DPPFNC systems

This section's objective is obtain the stability criterion of the event-triggered time delay DPPFNC system combined with the IT2-MFD method. It can be seen from (38) that the error terms $\Delta\underline{h}^*_{ijl}\left(\alpha^*_{ij}, \mathbf{x}(k)\right)$ and $\Delta\bar{h}^*_{ijl}\left(\beta^*_{ij}, \mathbf{x}(k)\right)$ within the subspace l exists such $\Delta\underline{h}^*_{ijl}(\alpha^*_{ijl}, \mathbf{x}) \le \left|\Delta\underline{h}^*_{ijl}(\alpha^*_{ijl}, \mathbf{x})\right| \le \left\|\Delta\underline{h}^*_{ijl}(\alpha^*_{ijl}, \mathbf{x})\right\|_\infty$ and $\Delta\bar{h}^*_{ijl}(\beta^*_{ijl}, \mathbf{x}) \le \left|\Delta\bar{h}^*_{ijl}(\beta^*_{ijl}, \mathbf{x})\right| \le \left\|\Delta\bar{h}^*_{ijl}(\beta^*_{ijl}, \mathbf{x})\right\|_\infty$, respectively. In addition, $\delta^*_{ijl}(\alpha^*_{ijl})$ is defined as a constant upper bound of $\Delta\underline{h}^*_{ijl}\left(\alpha^*_{ij}, \mathbf{x}(k)\right)$, satisfying $\delta^*_{ijl}(\alpha^*_{ijl}) \le \Delta\underline{h}^*_{ijl}(\alpha^*_{ijl}, \mathbf{x})$. Meanwhile, denote slack matrices $\mathbf{Y}_{ijl}(\mathbf{x})$, it holds that $\mathbf{Y}_{ijl}(\mathbf{x}) \ge 0 > \mathbf{Q}_{ij}(\mathbf{x})$, with $\forall i \in \underline{p}, \forall j \in \underline{c}, \forall l \in \underline{L}$. Then, from (22) and (34),

$$\Delta\mathbf{V}(\mathbf{x}(k)) = \sum_{i=1}^{p}\sum_{j=1}^{c}\sum_{l=1}^{L}\varsigma_l(\mathbf{x})\tilde{h}_{ijl}(\mathbf{x}(k), \mathbf{x}(k_\wp))\mathbf{Q}_{ij}(\mathbf{x})\mathbf{x}$$
$$\le \sum_{i=1}^{p}\sum_{j=1}^{c}\sum_{l=1}^{L}\varsigma_l(\mathbf{x})\Big(\underline{h}_{ijl}(\mathbf{x}(k), \mathbf{x}(k_\wp))\mathbf{Q}_{ij}(\mathbf{x}) + \Big(\bar{h}_{ijl}(\mathbf{x}(k), \mathbf{x}(k_\wp)) - \underline{h}_{ijl}(\mathbf{x}(k), \mathbf{x}(k_\wp))\Big)\mathbf{Y}_{ijl}(\mathbf{x})\Big)\mathbf{x}$$

$$\leq \sum_{i=1}^{p}\sum_{j=1}^{c}\sum_{l=1}^{L}\varsigma_l(\mathbf{x})\Big((\hat{\underline{h}}^*_{ijl}(\alpha^*_{ijl},\mathbf{x})+\delta^*_{ijl}(\alpha^*_{ijl}))\mathbf{Q}_{ij}(\mathbf{x})$$
$$+(\|\Delta\underline{h}^*_{ijl}(\alpha^*_{ijl},\mathbf{x})\|_\infty-\delta^*_{ijl}(\alpha^*_{ijl}))\mathbf{Y}_{ijl}(\mathbf{x})$$
$$+\Big((\hat{\bar{h}}^*_{ijl}(\beta^*_{ijl},\mathbf{x})+\|\Delta\bar{h}^*_{ijl}(\beta^*_{ijl},\mathbf{x})\|_\infty)$$
$$-(\hat{\underline{h}}^*_{ijl}(\alpha^*_{ijl},\mathbf{x})+\delta^*_{ijl}(\alpha^*_{ijl}))\Big)\mathbf{Y}_{ijl}(\mathbf{x})\Big)\mathbf{x}$$
$$=\sum_{i=1}^{p}\sum_{j=1}^{c}\sum_{l=1}^{L}\varsigma_l(\mathbf{x})\Big((\hat{\underline{h}}^*_{ijl}(\alpha^*_{ijl},\mathbf{x})+\delta^*_{ijl}(\alpha^*_{ijl}))\mathbf{Q}_{ij}(\mathbf{x})$$
$$+\Big(\hat{\bar{h}}^*_{ijl}(\beta^*_{ijl},\mathbf{x})-\hat{\underline{h}}^*_{ijl}(\alpha^*_{ijl},\mathbf{x})+\|\Delta\underline{h}^*_{ijl}(\alpha^*_{ijl},\mathbf{x})\|_\infty$$
$$+\|\Delta\bar{h}^*_{ijl}(\beta^*_{ijl},\mathbf{x})\|_\infty-2\delta^*_{ijl}(\alpha^*_{ijl})\Big)\mathbf{Y}_{ijl}(\mathbf{x})\Big)\mathbf{x}, \quad (41)$$

where $\underline{h}^*_{ijl}(\alpha^*_{ijl},\mathbf{x})$ is the approximation lower GA-MF, $\bar{h}^*_{ijl}(\beta^*_{ijl},\mathbf{x})$ is the approximation upper GA-MF. The optimum uniform norm $\left\|\Delta\underline{h}^*_{ijl}(\alpha^*_{ijl},\mathbf{x})\right\|_\infty$ and $\left\|\Delta\bar{h}^*_{ijl}(\beta^*_{ijl},\mathbf{x})\right\|_\infty$ obtained by GA are non-negative constants. Moreover, the GA-MFs information of different substate spaces is considered, and the state variable information is further considered, which makes the stability results more accurate:

$$\Delta\mathbf{V}(\mathbf{x}(k))\leq\sum_{i=1}^{p}\sum_{j=1}^{c}\sum_{l=1}^{L}\varsigma_l(\mathbf{x})\Big((\hat{\underline{h}}^*_{ijl}(\alpha^*_{ijl},\mathbf{x})+\delta^*_{ijl}(\alpha^*_{ijl}))$$
$$\times\mathbf{Q}_{ij}(\mathbf{x})+\Big(\hat{\bar{h}}^*_{ijl}(\beta^*_{ijl},\mathbf{x})-\hat{\underline{h}}^*_{ijl}(\alpha^*_{ijl},\mathbf{x})+\|\Delta\underline{h}^*_{ijl}(\alpha^*_{ijl},\mathbf{x})\|_\infty$$
$$+\|\Delta\bar{h}^*_{ijl}(\beta^*_{ijl},\mathbf{x})\|_\infty-2\delta^*_{ijl}(\alpha^*_{ijl})\Big)\mathbf{Y}_{ijl}(\mathbf{x})$$
$$+\sum_{\kappa=1}^{n}(x_\kappa(k)-x_{\kappa l\min})(x_{\kappa l\max}-x_\kappa(k))\mathbf{R}_{\kappa l}(\mathbf{x})\Big)\mathbf{x}, \quad (42)$$

where $x_{\kappa l\min}\leq x_\kappa(k)\leq x_{\kappa l\max}$ in the lth subspace. Slack scalar $\mathbf{R}_{\kappa l}(\mathbf{x})$ satisfy the condition $\mathbf{R}_{\kappa l}(\mathbf{x})\geq 0$, $\forall\kappa\in\underline{n},\forall l\in\underline{L}$.

Based on IT2-MFD, the following theorem states the positivity and stability conditions of SOS form that ensure the positivity and stability of the time delay DPPFNC system (15).

Theorem 2: For time delay DPPFNC system (15) under the ETC scheme (8), if there exist prescribed positive scalars $0<\gamma\leq 1$, vectors $y^{ijl}_s(\mathrm{x})$, $r^{\kappa l}_s(\mathrm{x})$ and λ, $\boldsymbol{\theta}_s$, $\boldsymbol{\phi}_s\in\Re^n$ make the following SOS conditions hold with $i\in\underline{p}$, $j\in\underline{c}$, $l\in\underline{L}$ and $\kappa,s\in\underline{n}$:

$$\lambda_s-\varepsilon_1 \text{ is SOS}; s\in\underline{n}, \quad (43)$$

$$y^{ijl}_s(\mathbf{x}(k)) \text{ is SOS}; s\in\underline{n}, \quad (44)$$

$$a^{\tau i}_{fs}(\mathbf{x}(k)) \text{ is SOS}; i\in\underline{p}, f=s\in\underline{n}, \quad (45)$$

$$m^{ij+}_s(\mathbf{x}(k))-\varepsilon_2(\mathbf{x}(k)) \text{ is SOS}; s\in\underline{n}, \quad (46)$$

$$-(m^{ij-}_s(\mathbf{x}(k))+\varepsilon_2(\mathbf{x}(k))) \text{ is SOS}; s\in\underline{n}, \quad (47)$$

$$y^{ijl}_s(\mathbf{x}(k))-q^{ij}_s(\mathbf{x}(k) \text{ is SOS}; i\in\underline{p}, j\in\underline{c}, l\in\underline{L}, s\in\underline{n}, \quad (48)$$

$$\lambda^T\mathbf{B}_i(\mathbf{x}(k))\mathbf{I}_m a^i_{fs}(\mathbf{x}(k))+\mathbf{b}^i_f(\mathbf{x}(k))\mathbf{I}_m\mathbf{M}^+_{ij}(\mathbf{x}(k))\boldsymbol{\theta}_s$$
$$+\mathbf{b}^i_f(\mathbf{x}(k))\mathbf{I}_m\mathbf{M}^-_{ij}(\mathbf{x}(k))\boldsymbol{\phi}_s \text{ is SOS}; i\in\underline{p}, j\in\underline{c}, f,s\in\underline{n}, \quad (49)$$

$$-\Bigg(\sum_{i=1}^{p}\sum_{j=1}^{c}\Big(((\hat{\underline{h}}^*_{ijl}(\alpha^*_{ijl},\mathbf{x})+\delta^*_{ijl}(\alpha^*_{ijl}))q^{ij}_s(\mathbf{x})$$
$$+\Big(\hat{\bar{h}}^*_{ijl}(\beta^*_{ijl},\mathbf{x})-\hat{\underline{h}}^*_{ijl}(\alpha^*_{ijl},\mathbf{x})+\|\Delta\underline{h}^*_{ijl}(\alpha^*_{ijl},\mathbf{x})\|_\infty$$
$$+\|\Delta\bar{h}^*_{ijl}(\beta^*_{ijl},\mathbf{x})\|_\infty-2\delta^*_{ijl}(\alpha^*_{ijl})\Big)y^{ijl}_s(\mathbf{x}(k))$$
$$+\sum_{\kappa=1}^{n}(x_\kappa(k)-x_{\kappa l\min})(x_{\kappa l\max}-x_\kappa(k))r^{\kappa l}_s(\mathbf{x}(k))\Big)$$
$$+\varepsilon_2(\mathbf{x}(k)))\Bigg) \text{ is SOS}; i\in\underline{p}, j\in\underline{c}, l\in\underline{L}, \kappa,s\in\underline{n}, \quad (50)$$

in which $\mathbf{Y}_{ijl}(\mathbf{x}(k))=[y^{ijl}_1(\mathbf{x}(k)),y^{ijl}_2(\mathbf{x}(k)),...,y^{ijl}_n(\mathbf{x}(k))]^T$; $\mathbf{R}_{\kappa l}(\mathbf{x}(k))=[r^{\kappa l}_1(\mathbf{x}(k)),r^{\kappa l}_2(\mathbf{x}(k)),...,r^{\kappa l}_n(\mathbf{x}(k))]^T$, $\forall i\in\underline{p}$, $j\in\underline{c}$, $\forall\kappa\in\underline{n}$, $l\in\underline{L}$. Theorem 1 shows the $q^{ij}_s(\mathbf{x}(k))$, (25) shows the event-triggered feedback gains. $\hat{\underline{h}}^*_{ijl}(\alpha^*_{ijl},\mathbf{x})$, $\hat{\bar{h}}^*_{ijl}(\alpha^*_{ijl},\mathbf{x})$ and $\left\|\Delta\underline{h}^*_{ijl}(\alpha^*_{ijl},\mathbf{x})\right\|_\infty$, $\left\|\Delta\bar{h}^*_{ijl}(\beta^*_{ijl},\mathbf{x})\right\|_\infty$ are the lower, upper GA-MFs and the best uniform norm between the original lower, upper IT2-MFs and the lower, upper GA-MFs within lth subspace.

Remark 11: The upper and lower MFs successfully capture parameter uncertainties with the IT2 fuzzy sets. Therefore, to consider the IT2 MFs in relaxation stability analysis, GA is first used to optimize the approximation polynomial of the IT2-MFs, which realizes the combination of traditional numerical field and evolutionary intelligence algorithm. In addition, to avoid the Runge phenomenon, the uniform norm is introduced into the space, and the approximate polynomials with the minimum uniform norm form errors from the original MFs are obtained.

Remark 12: Due to the introduction of ETC mechanism, IT2 fuzzy model premise variable $\mathbf{x}(k)$ is different from fuzzy controller premise variable $\mathbf{x}(k_\wp)$, which leads to $\tilde{h}_{ij}(\mathbf{x}(k),\mathbf{x}(k_\wp))$ dependents on $\mathbf{x}(k)$ and $\mathbf{x}(k_\wp)$. According to the ET condition (8), it can be seen that there is a specific constraint between $\mathbf{x}(k)$ and $\mathbf{x}(k_\wp)$. Assuming that $\mathbf{x}(k)$ and $\mathbf{x}(k_\wp)$ are independent variables, some information about the MF will inevitably be lost, leading to conservative stability conditions. To introduce more information about $m_j(\mathbf{x}(k_\wp))$, the constraint between $\mathbf{x}(k)$ and $\mathbf{x}(k_\wp)$ is applied to further estimate $m_j(\mathbf{x}(k_\wp))$ by $m_j(\mathbf{x}(k))$, and the MFs depend on the only variable $\mathbf{x}(k)$. Therefore, based on the ET condition (8), this estimation is achieved by finding the constraint between $\mathbf{x}(k)$ and $\mathbf{x}(k_\wp)$ during the sampling period. From (7) and (16), the following inequation is given:

$$-\gamma\mathbf{1}_{n\times n}\mathbf{x}(k)\leq\mathbf{x}(k_\wp)-\mathbf{x}(k)\leq\gamma\mathbf{1}_{n\times n}\mathbf{x}(k). \quad (51)$$

Thus, the estimate of $\mathbf{x}(k_\wp)$ is obtained by means of the following condition:

$$\mathbf{x}(k_\wp)\in[\boldsymbol{\Theta}\mathbf{x}(k),\boldsymbol{\Phi}\mathbf{x}(k)]. \quad (52)$$

The aforementioned conclusion can be summed up in the following lemma.

Lemma 3: Given any $\mathbf{x}(k)$, there exists an inequality between the mismatching $\mathbf{x}(k)$ and $\mathbf{x}(k_{\wp})$ represented by parameters $\mathbf{\Theta}$ and $\mathbf{\Phi}$ during the sampling period.

$$\mathbf{x}(k_{\wp}) = [\mathbf{\Theta}\mathbf{x}(k), \mathbf{\Phi}\mathbf{x}(k)],$$

where $\mathbf{\Theta} = \mathbf{I} - \gamma \mathbf{1}_{n\times n}$, $\mathbf{\Phi} = \mathbf{I} + \gamma \mathbf{1}_{n\times n}$.

IV. Simulation Example

For the IT2 event-trigger-based DPPFNC system with time delay, the usefulness and excellence of SOS-based stability criterion and event-based network control methods are verified by examples.

A. A Numerical Example

The parameters of the example of the DPPFNC system with a 3-rule polynomial fuzzy model are chosen as follows for the $\mathbf{x}(k) = [x_1(k)\ x_2(k)]^T$.

$$\mathbf{A}_1(x_1(k)) = \begin{bmatrix} 0.85 & 0.609 + 0.012x_1 + 0.0005x_1^2 \\ 0.20 & 0.385 \end{bmatrix},$$

$$\mathbf{A}_2(x_1(k)) = \begin{bmatrix} 0.40 + 0.001x_1^2 & 0.434 \\ 0.34 & 0.406 + 0.004x_1 + 0.001x_1^2 \end{bmatrix},$$

$$\mathbf{A}_3(x_1(k)) = \begin{bmatrix} 0.51 + 0.001x_1^2 & 0.315 + 0.08a \\ 0.50 + 0.013x_1 + 0.002x_1^2 & 0.453 + 0.02b \end{bmatrix},$$

$$\mathbf{B}_1 = \begin{bmatrix} 1.20 \\ 0 \end{bmatrix}, \mathbf{B}_2 = \begin{bmatrix} 0.68 \\ 0 \end{bmatrix}, \mathbf{B}_3 = \begin{bmatrix} 0.66 + 0.02b \\ 0 \end{bmatrix},$$

$$\mathbf{A}_{\tau 1}(x_1(k)) = \begin{bmatrix} 0.001 & 0.001x_1^2(k) \\ 0 & 0 \end{bmatrix},$$

$$\mathbf{A}_{\tau 2}(x_1(k)) = \begin{bmatrix} 0.003 & 0.004 + 0.001x_1^2(k) \\ 0 & 0 \end{bmatrix},$$

$$\mathbf{A}_{\tau 3}(x_1(k)) = \begin{bmatrix} 0 & 0.002 + 0.0005x_1^2(k) \\ 0 & 0 \end{bmatrix},$$

in which a and b are constant system parameters. The IT2 polynomial fuzzy model MFs are selected being $\underline{w}_1(x_1) = 1 - 1/\left(1 + e^{(-x_1+4.5)}\right)$, $\underline{w}_3(x_1) = 1/\left(1 + e^{(-x_1+15.5)}\right)$, $\overline{w}_2(x_1) = 1 - \underline{w}_1(x_1) - \underline{w}_3(x_1)$, $\overline{w}_1(x_1) = 1 - 1/\left(1 + e^{(-x_1+5)}\right)$, $\overline{w}_3(x_1) = 1/\left(1 + e^{(-x_1+15)}\right)$, and $\underline{w}_2(x_1) = 1 - \overline{w}_1(x_1) - \overline{w}_3(x_1)$. From (5), we have $\tilde{w}_1(\mathbf{x}(k)) = \underline{\lambda}_1(\mathbf{x}(k))w_1^L(\mathbf{x}(k)) + \bar{\lambda}_i(\mathbf{x}(k))w_i^U(\mathbf{x}(k))$ for $i \in [1, 2, 3]$, where the nonlinear type reduction functions are chosen as $\underline{\lambda}_1(x_1) = (\sin(2x_1) + 2)/3$, $\bar{\lambda}_1(x_1) = 1 - (\sin(2x_1) + 2)/3$, $\underline{\lambda}_3(x_1) = (\cos(2x_1) + 2)/3$ and $\bar{\lambda}_3(x_1) = 1 - (\cos(2x_1) + 2)/3$. After $\tilde{w}_1(x(k))$ and $\tilde{w}_3(x(k))$ are determined, $\tilde{w}_2(x(k))$ can be obtained using the properties of MF $\sum_{i=1}^{p} \tilde{w}_i(x(k)) = 1$.

Under the IPM design, the two-rule IT2 event-triggered fuzzy controller MFs are selected being $\underline{m}_1(x_1) = 1 - 1/\left(1 + e^{(-(1-\gamma)x_1+9.8)}\right)$, $\overline{m}_2(x_1) = 1 - \underline{m}_1(x_1)$, $\overline{m}_1(x_1) = 1 - 1/\left(1 + e^{(-(1+\gamma)x_1+10.2)}\right)$, and $\underline{m}_2(x_1) = 1 - \overline{m}_1(x_1)$. Due to the introduction of an ETC scheme (8), only the state $\mathbf{x}(k_{\wp})$ at the triggering instant $k_{\wp}(\wp = 1, 2, ...)$ is observed by the controller, which leads to a mismatch between the nonlinear plant and the controller's MF premise variables. Therefore, we estimate the upper and lower bounds of the IT2 MF $\tilde{m}_j(\mathbf{x}(k_{\wp}))$ of the controller by the minimum value of $\underline{m}_j(\mathbf{x}(k))$ and the maximum value of $\overline{m}_j(\mathbf{x}(k))$ in the relation interval $[\mathbf{\Theta}\mathbf{x}(k), \mathbf{\Phi}\mathbf{x}(k)]$ of $\mathbf{x}(k)$ and $\mathbf{x}(k_{\wp})$ in Lemma 3. From (13), the type reduction functions $\underline{\kappa}_j(x(k_{\wp})) = \overline{\kappa}_j(x(k_{\wp})) = \frac{1}{2}$, for $j = 1, 2$.

Suppose the operating domain is $x_1 \in [0, 10]$ and uniformly divide the x_1 into 5 subdomains ($L = 5$); we have $x_{\kappa l\min} \leq x_1 \leq x_{\kappa l\max}$, $l = 1, 2, ..., 5$, where $x_{\kappa l\min} = k$ and $x_{\kappa l\max} = k + 2$.

TABLE I
GA-MFs of Different Orders and Subdomains

Case	Order	Subdomain
1	2	$[0, 5), [5, 10]$
2	0	$[0, 2), [2, 4), [4, 6), [6, 8), [8, 10]$
3	2	$[0, 2), [2, 4), [4, 6), [6, 8), [8, 10]$

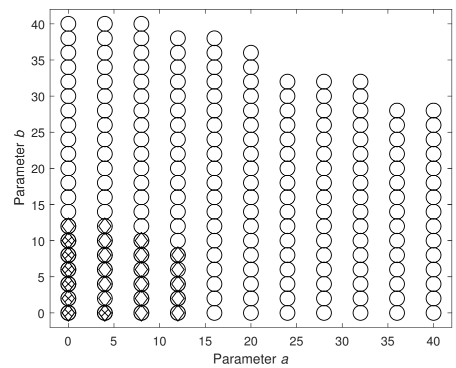

Fig. 1. Stabilization regions derived from Theorem 2 with $\mathbf{Y}_{ij}(\mathbf{x}(k))$ of degree 0 to 2 and $\mathbf{R}_{ij}(x(k))$ of degree 0 to 2, indicated by "$\times$" for Case 1, and "$\diamond$" for Case 2, and "$\circ$" for Case 3 in Example 1.

Example1: According to Theorem 2, SOS-based stability criteria are used to verify the stability of the IT2 event-trigger-based DPPFNC system with time delay under the $0 \leq a \leq 40$ at the period of 4 and $0 \leq b \leq 40$ at the period of 2 to ensure the usefulness of the approach method. In the simulation, we set $\varepsilon_1 = \varepsilon_2 = 1 \times 10^{-3}$; $\mathbf{M}_{ij}(\mathbf{x}(k_{\wp}))$ as constant matrix, slack matrix $\mathbf{Y}_{ij}(\mathbf{x}(k))$ and $\mathbf{R}_{ij}(\mathbf{x}(k))$ as polynomial of degree 0 to 2 in x_1. Referring to Theorem 2, the original MF is approximated by GA. The control parameters of GA satisfy coding length $s = 10$, population size $N = 100$, crossover and mutation probability $p_c = 0.8$, $p_m = 0.001$ and termination condition $T < 100$. From three cases, we consider GA-MFs of different orders and intervals of subdomain in Table I. Fig. 1 shows stabilization regions derived from Theorem 2 with $\mathbf{Y}_{ij}(\mathbf{x}(k))$ of degree 0 to 2 and $\mathbf{R}_{ij}(x(k))$ of degree 0 to 2, indicated by "$\times$" for Case 1, and "$\diamond$" for Case 2, and "$\circ$" for Case 3.

The role of slack matrix $\mathbf{Y}_{ij}(\mathbf{x}(k))$ and $\mathbf{R}_{ij}(x(k))$ are verified from Fig. 2 on the stability domain, the stability

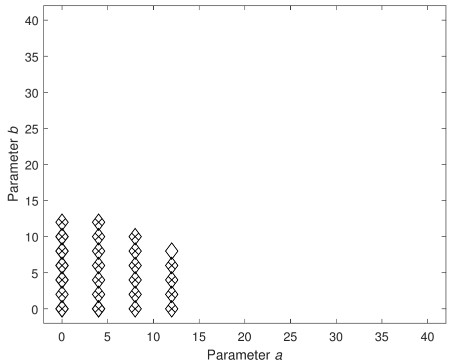

Fig. 2. Stabilization regions of Case 2 derived from Theorem 2 with $\mathbf{Y}_{ij}(\mathbf{x}(k))$ of degree 0 and $\mathbf{R}_{ij}(x(k))$ of degree 0 indicated by "$\circ$", $\mathbf{Y}_{ij}(\mathbf{x}(k))$ of degree 0 to 2 and $\mathbf{R}_{ij}(x(k))$ of degree 0 indicated by "$\times$", $\mathbf{Y}_{ij}(\mathbf{x}(k))$ of degree 0 to 2 and $\mathbf{R}_{ij}(x(k))$ of degree 0 to 2 indicated by "$\diamond$"in Example 1.

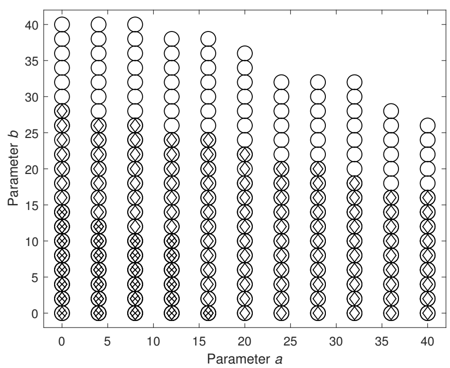

Fig. 3. Stabilization regions of Case 2 derived from Theorem 2, indicated by "$\times$" for event-triggered threshold parameter $\gamma = 0.45$, "$\diamond$" for event-triggered threshold parameter $\gamma = 0.40$ and "$\circ$" for event-triggered threshold parameter $\gamma = 0.35$ in Example 2.

regions of Case 2 are indicated by "$\circ$" with $\mathbf{Y}_{ij}(\mathbf{x}(k))$ of degree 0 and $\mathbf{R}_{ij}(x(k))$ of degree 0, "$\times$" with $\mathbf{Y}_{ij}(\mathbf{x}(k))$ of degree 0 to 2 and $\mathbf{R}_{ij}(x(k))$ of degree 0 and "$\diamond$" with $\mathbf{Y}_{ij}(\mathbf{x}(k))$ of degree 0 to 2 and $\mathbf{R}_{ij}(x(k))$ of degree 0 to 2, respectively.

According to Fig. 1, the higher the order of GA-MFs, the smaller subdomain, leading to a larger stabilization region, which is for case 1 to case 3. In addition, Fig. 2 shows that the higher degree slack matrixes $\mathbf{Y}_{ij}(\mathbf{x}(k))$ and $\mathbf{R}_{ij}(\mathbf{x}(k))$ always provide a larger stabilization region than the lower degree slack matrixes. It verifies that the operating domain information and slack matrix $\mathbf{Y}_{ij}(\mathbf{x}(k))$ and $\mathbf{R}_{ij}(\mathbf{x}(k))$ are effective for relaxing stability conditions.

Example2: In this example, we discuss the effect of the event-triggered threshold value γ on the stability domain and the number of event-triggered instants. Parameters a and b are same as in Example 1 to verify the stability of the time delay IT2 event-trigger-based DPPFNC system. $\mathbf{M}_{ij}(\mathbf{x}(k_\wp))$ are defined in Example 1. Slack matrixes $\mathbf{Y}_{ij}(\mathbf{x}(k))$ and $\mathbf{R}_{ij}(\mathbf{x}(k))$ as polynomial of degree 0 to 2 in x_1; GA-MFs as approximate polynomials of order 2 and interval 2 in the overall domain. The stability regions corresponding to event-triggered threshold parameter in Fig. 3, $\gamma = 0.45, 0.40, 0.35$ indicated by "$\times$", "$\diamond$" and "$\circ$", respectively. Fig. 3 shows that on the premise that the value of event-triggered threshold parameter γ can make Theorem 2 have a feasible solution, the smaller of γ, the larger the range of stabilisation points.

TABLE II
SOME RESULTS FOR DIFFERENT VALUE OF γ

Value γ	NPRχ (DRRp%)	Feedback gains G_1, G_2
0.44	14(66.67%)	$\begin{bmatrix} G_1 \\ G_2 \end{bmatrix} = \begin{bmatrix} -0.4053, -0.0028 \\ -0.4029, -0.0050 \end{bmatrix}$
0.43	14(66.67%)	$\begin{bmatrix} G_1 \\ G_2 \end{bmatrix} = \begin{bmatrix} -0.4058, -0.0049 \\ -0.3996, -0.0113 \end{bmatrix}$
0.35	16(76.19%)	$\begin{bmatrix} G_1 \\ G_2 \end{bmatrix} = \begin{bmatrix} -0.3994, -0.0713 \\ -0.3528, -0.1982 \end{bmatrix}$
0.33	17(80.95%)	$\begin{bmatrix} G_1 \\ G_2 \end{bmatrix} = \begin{bmatrix} -0.3984, -0.0965 \\ -0.3423, -0.2150 \end{bmatrix}$
0.32	18(85.71%)	$\begin{bmatrix} G_1 \\ G_2 \end{bmatrix} = \begin{bmatrix} -0.3977, -0.1102 \\ -0.3375, -0.2221 \end{bmatrix}$
0.30	19(90.48%)	$\begin{bmatrix} G_1 \\ G_2 \end{bmatrix} = \begin{bmatrix} -0.3965, -0.1392 \\ -0.3292, -0.2344 \end{bmatrix}$

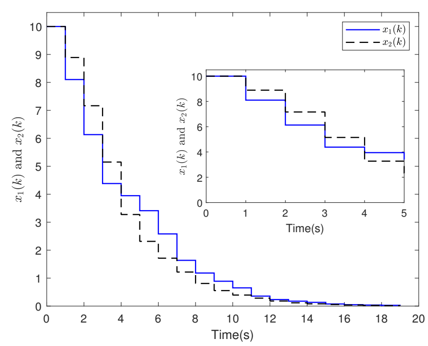

Fig. 4. Time response of system with the initial state $[10, 10]$ for Case 3, the dashed line represents time response of $x_1(k)$, the solid line represents time response of $x_2(k)$.

To illustrate the influence of different event-triggered threshold parameters γ of the ETC scheme on the event-trigger times, the system parameters $a = 12$ and $b = 10$ of Case 3 were selected for simulation. $\mathbf{M}_{ij}(\mathbf{x}(k_\wp))$ are defined in Example 1. Slack matrixs $\mathbf{Y}_{ij}(\mathbf{x}(k))$ and $\mathbf{R}_{ij}(\mathbf{x}(k))$ as polynomials of degree 0 to 2 in x_1. In Table II shows some calculation results under different ET threshold γ, where χ denotes the number of packet releasing (NPR), $p(\%)$ denotes the data releasing rate (DRR). And the number of data sampling (NDS) is 21 within 21s, where DRR = $\frac{NPR}{NDS}$. Table II shows event-triggered times decrease with the increase of the ET threshold value γ and the conditions have no solutions when the ET threshold value γ exceeds a threshold. Observing the event-triggered condition can also draw a similar conclusion (8). When the event-triggered threshold γ is large, the ETC condition (8) is harder to violate, and the sampled states will continue to be maintained without updating the control input, to reduce the transmission of unnecessary data effectively.

Example3: Furthermore, in Fig.1, to illustrate the effectiveness of the ETC scheme, the system parameters $a = 40$ and $b = 28$ of Case 3 were selected for simulation.

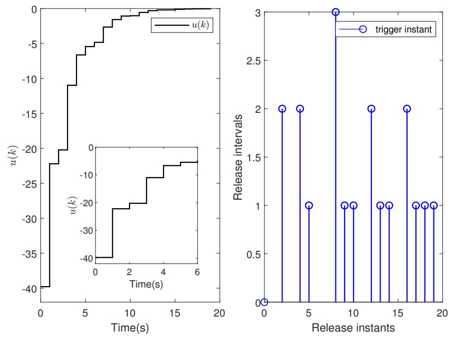

Fig. 5. Left: the event-triggered control input for Case 3; right: the release instants and release interval of the event-triggered control process for Case 3.

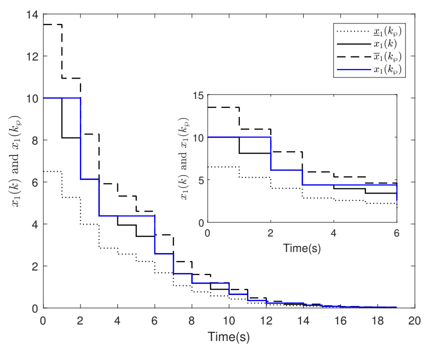

Fig. 6. Time response of $x(k_\wp)$ for Case 3. The solid black line, dotted black line, dashed black line and solid blue line represents $x_1(k)$, the lower bound for $x_1(k_\wp)$ utilizing the data from $x_1(k)$, the upper bound for $x_1(k_\wp)$ utilizing the data from $x_1(k)$ and $x_1(k_\wp)$, respectively.

The the IT2 fuzzy event-triggered controller gains in Case 3 are $G_1 = [-0.3065, -0.0092]$; $G_2 = [-0.2848, -0.0914]$ when the stability criterion of SOS form in Theorem 2 are resolved using the MATLAB toolbox SOSTOOLS. To visually display the stabilization effect of the designed event-triggered controllers in Case 3, the state response curves of the time delay IT2 event-trigger-based DPPFNC system under the initial condition $\mathrm{x}(0) = [10, 10]^T$ and event-triggered threshold $\gamma = 0.35$ are plotted in Fig.4. The time response curve over a specific period is expanded and set in the matching small window to present the simulation results more clearly. In Fig.4, the state variables $x_1(k)$ and $x_2(k)$ are stable at the equilibrium point, and the trajectories are always in the positive quadrant. So the positivity and stability of $\mathbf{x}(k)$ can be guaranteed.

In Fig.5, the ETC input and the triggered instants of the ETC process for Case 3 are displayed. Following that, we discover that only $14(66.67\%)$ times within $21s$ are transferred across the communication network. In other words, the planned ETC method can conserve scarce network resources. The link between $x(k)$ and $x(k_\wp)$ in Case 3 further demonstrates that it fulfils the derivation of lemma 3.

B. A Pest Population Example

A pest population example in [41] is considered in the following state space form:

$$\begin{aligned}
&\mathbf{A}(k) = \\
&\begin{bmatrix} 2+0.1\sin^2(x_1(k)) & 2.1+0.01\cos^2(x_1(k)) & 1.837 \\ 0.05 & 0 & 0 \\ 0 & 0.09 & 0 \end{bmatrix}, \\
&\mathbf{A}_\tau(k) = \\
&\begin{bmatrix} 0.08+0.01\cos^2(x_1(k)) & 0.04+0.01\sin^2(x_1(k)) & 0.04 \\ 0.04 & 0 & 0 \\ 0 & 0.04 & 0 \end{bmatrix}, \\
&\mathbf{B}(k) = \begin{bmatrix} 0.1+0.005\sin^2(x_1(k)) \\ 0 \\ 0 \end{bmatrix}, \tau = \left|\sin(\frac{\pi}{2}k)\right| + 1.
\end{aligned} \tag{53}$$

$\mathbf{x}(k) = [x_1(k), x_2(k), x_3(k)]^T$, $x_1(k)$, $x_2(k)$ and $x_3(k)$ denotes the number of juvenile pests, immature pests and adult pests considering time k.

It is assumed that the number of juvenile pests is greatly affected by the natural enemies of pests and the living environment, and these differences cannot be ignored, so the parameters cannot be accurately identified when modelling this system. Therefore, the above system is represented as a system with uncertain parameter Δa.

$$\begin{aligned}
&\mathbf{A}(k) = \\
&\begin{bmatrix} \begin{pmatrix} 0.1\sin^2(x_1(k)) \\ -\Delta a + 2 \end{pmatrix} & \begin{pmatrix} 0.01\cos^2(x_1(k)) \\ +0.1\Delta a + 2.1 \end{pmatrix} & 1.837 \\ 0.05 & 0 & 0 \\ 0 & 0.09 & 0 \end{bmatrix}, \\
&\mathbf{A}_\tau(k) = \\
&\begin{bmatrix} \begin{pmatrix} 0.01\cos^2(x_1(k)) \\ +0.1\Delta a + 0.08 \end{pmatrix} & \begin{pmatrix} 0.01\sin^2(x_1(k)) \\ -0.1\Delta a + 0.04 \end{pmatrix} & 0.04 \\ 0.04 & 0 & 0 \\ 0 & 0.04 & 0 \end{bmatrix}, \\
&\mathbf{B}(k) = \begin{bmatrix} 0.1+0.005\sin^2(x_1(k)) - 0.05\Delta a \\ 0 \\ 0 \end{bmatrix}.
\end{aligned} \tag{54}$$

First, we employ the sector nonlinearity method to approximate the pest population system using a fuzzy model. Consider the states $x_1(k) \in \left[0, \frac{\pi}{2}\right]$, $x_2(k) \in \left[0, \frac{\pi}{2}\right]$, $x_3(k) \in \left[0, \frac{\pi}{2}\right]$ according to the knowledge on this application and taking $f(x_1(k)) = 0.1\sin^2(x_1(k)) - \Delta a$ in the system matrix as nonlinearity term, then $f(x_1(k)) = \tilde{w}_1(x_1(k)) f_{\max} + \tilde{w}_2(x_1(k)) f_{\min}$, we have $\tilde{w}_1(x_1(k)) = \frac{f(x_1(k)) - f_{\min}}{f_{\max} - f_{\min}}$ and $\tilde{w}_2(x_1(k)) = 1 - \tilde{w}_1(x_1(k))$. f_{max} and f_{min} are the maximum and minimum values of $f(x_1(k))$ in the operating domain of states, respectively.

Considering Δa ($1 = \Delta a_{min} \leq \Delta a \leq \Delta a_{max} = 1.5$) to be an uncertain value, then $f_{max} = -0.9$ and $f_{min} = -1.5$, the lower and upper MFs of a model under $x_1(k) \in \left[0, \frac{\pi}{2}\right]$ are $\overline{w}_1(x_1(k)) = \frac{0.1\sin^2(x_1(k)) - \Delta a_{\min} - f_{\min}}{f_{\max} - f_{\min}}$, $\underline{w}_1(x_1(k)) = \frac{0.1\sin^2(x_1(k)) - \Delta a_{\max} - f_{\min}}{f_{\max} - f_{\min}}$, $\underline{w}_2(x_1(k)) = 1 - \overline{w}_1(x_1(k))$ and

$\overline{w}_2(x_1(k)) = 1 - \underline{w}_1(x_1(k))$. Then, the system and input matrices are determined as follows:

$$\mathbf{A}_1(k) = \begin{bmatrix} 1.1 & 2.2 & 1.837 \\ 0.05 & 0 & 0 \\ 0 & 0.09 & 0 \end{bmatrix}, \mathbf{B}_1(k) = \begin{bmatrix} 0.055 \\ 0 \\ 0 \end{bmatrix}$$
$$\mathbf{A}_2(k) = \begin{bmatrix} 0.5 & 2.26 & 1.837 \\ 0.05 & 0 & 0 \\ 0 & 0.09 & 0 \end{bmatrix}, \mathbf{B}_2(k) = \begin{bmatrix} 0.025 \\ 0 \\ 0 \end{bmatrix}$$
$$\mathbf{A}_{\tau 1}(k) = \begin{bmatrix} 0.18 & 0.03 & 0.04 \\ 0.04 & 0 & 0 \\ 0 & 0.04 & 0 \end{bmatrix},$$
$$\mathbf{A}_{\tau 2}(k) = \begin{bmatrix} 0.24 & 0.025 & 0.04 \\ 0.04 & 0 & 0 \\ 0 & 0.04 & 0 \end{bmatrix}. \quad (55)$$

The frequent use of agrochemical will destroy the ecological environment and bring a particular waste of human and material resources. Therefore, this paper adopts the ETC strategy to rationally arrange the days of agrochemical use, which can not only achieve the balance of pest populations in this environment but also reduce the waste of resources. The lower and upper MFs of controller are chosen as $\underline{m}_1(x_1(k)) = e^{-\left(x_1(k)-\frac{\pi}{4}\right)^2/0.05}$, $\overline{m}_1(x_1(k)) = e^{-\left(x_1(k)-\frac{\pi}{4}\right)^2/0.1}$, $\overline{m}_2(x_1(k)) = 1 - \underline{m}_1(x_1(k))$ and $\underline{m}_2(x_1(k)) = 1 - \overline{m}_1(x_1(k))$.

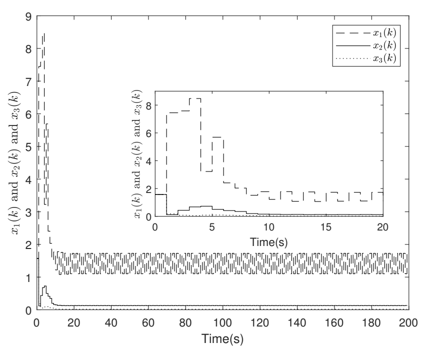

Fig. 7. Time response of $x_1(k)$ (dashed lines), $x_2(k)$ (solid lines) and $x_3(k)$ (dotted lines) of open-loop system with the initial state $x(0) = \left[\frac{\pi}{2}, \frac{\pi}{2}, \frac{\pi}{2}\right]^T$.

In Fig. 7, the open-loop pest population system is unstable, which means that the pest population is unbalanced in this ecosystem. In the following, the SOS-based stability conditions in Theorem 1 under the ET threshold parameter $\gamma = 0.1$ are employed to verify the system positivity and stability. The state response curves of the pest population under the initial condition $x(0) = \left[\frac{\pi}{2}, \frac{\pi}{2}, \frac{\pi}{2}\right]^T$ are plotted in Fig. 8. The state variables are stable at equilibrium, and the trajectories are always in the positive quadrant. The feedback gains are $G_1 = [-16.5608, -3.3895, -0.9637]$, $G_2 = [-16.5608, -3.3895, -0.9637]$. The triggered instants of the ETC process are plotted in Fig. 9. Only $19(90.48\%)$ out of 21 days of agrochemical treatment is needed. It means that the ETC scheme can save resources while ensuring the stability of pest populations.

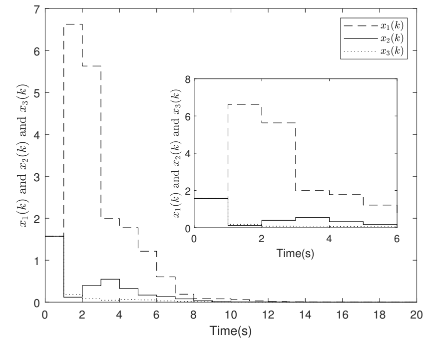

Fig. 8. Time response of $x_1(k)$ (dashed lines), $x_2(k)$ (solid lines) and $x_3(k)$ (dotted lines) of pest population system given by Theorem 1 with the initial state $x(0) = \left[\frac{\pi}{2}, \frac{\pi}{2}, \frac{\pi}{2}\right]^T$.

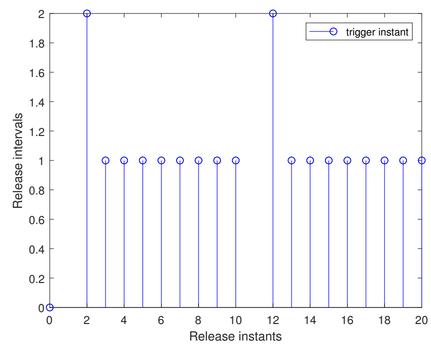

Fig. 9. The release instants and release interval of the event-triggered control process.

Remark 13: The stability criterion established by Theorem 1 are also used in a simulation instance to demonstrate the superiority of the provided MFD approach. It is discovered that the value range of $0 \le a \le 40$ and $0 \le b \le 40$ does not contain a stable point of Theorem 1. Therefore, it fully demonstrated that the MFD method can effectively relax and stabilize conditions to obtain a larger stability domain.

V. Conclusion

This paper analyzes the stability and positivity of the time delay IT2 DPPFNC system with asynchronous premises and the ETC scheme. The sufficiency requirements in SOS form are obtained from the IT2 polynomial fuzzy model based on the LCLF, and the IT2 polynomial fuzzy event-triggered controller is created using the IPM principle. The 1-norm ETC is adopted to lower the DPPFNC systems with time-delay communication energy consumption. A GA-MFD approach to optimize the approximation error of IT2 MFs was presented to attain a broader range of stable spots. This approach is based on the principle of the optimum uniform approximation.

References

[1] S. Xiao, Q. L. Han, X. Ge, and Y. Zhang, "Secure distributed finite-time filtering for positive systems over sensor networks under deception attacks," *IEEE transactions on cybernetics*, vol. 50, no. 3, pp. 1220–1229, 2019.

[2] Y. Wu, J. Zhang, and P. Lin, "Non-fragile hybrid-triggered control of networked positive switched systems with cyber attacks," *Physica A: Statistical Mechanics and its Applications*, vol. 588, p. 126571, 2022.

[3] J. J. Liu, K.-W. Kwok, Y. Cui, J. Shen, and J. Lam, "Consensus of positive networked systems on directed graphs," *IEEE Transactions on Neural Networks and Learning Systems*, 2021.

[4] Y.-W. Wang, Z.-H. Zeng, X.-K. Liu, and Z.-W. Liu, "Input-to-state stability of switched linear systems with unstabilizable modes under dos attacks," *Automatica*, vol. 146, p. 110607, 2022.

[5] L. Benvenuti and L. Farina, "Positive and compartmental systems," *IEEE Transactions on Automatic Control*, vol. 47, no. 2, pp. 370–373, 2002.

[6] S. Xiao, Q. L. Han, X. Ge, and Y. Zhang, "Secure distributed finite-time filtering for positive systems over sensor networks under deception attacks," *IEEE Transactions on Cybernetics*, pp. 1–10, 2020.

[7] J. Zhang, S. Zhang, and P. Lin, "Event-triggered model predictive control of positive systems with random actuator saturation," *Nonlinear Dynamics*, p. 417–437, 2021.

[8] H. Arneson and C. Langbort, "A linear programming approach to routing control in networks of constrained linear positive systems," *Automatica*, vol. 48, no. 5, pp. 800–807, 2012.

[9] P. Chen, W. Min, X. Xie, and Y. L. Wang, "Event-triggered predictive control for networked nonlinear systems with imperfect premise matching," *IEEE Transactions on Fuzzy Systems*, vol. PP, no. 5, pp. 1–1, 2018.

[10] Z. Cao, B. Niu, G. Zong, and N. Xu, "Small-gain technique-based adaptive output constrained control design of switched networked nonlinear systems via event-triggered communications," *Nonlinear Analysis: Hybrid Systems*, vol. 47, p. 101299, 2023.

[11] F. Cheng, H. Liang, H. Wang, G. Zong, and N. Xu, "Adaptive neural self-triggered bipartite fault-tolerant control for nonlinear MASs with dead-zone constraints," *IEEE Transactions on Automation Science and Engineering*, pp. 1–12, 2022.

[12] X. Zhao, X. Wang, L. Ma, and G. Zong, "Fuzzy approximation based asymptotic tracking control for a class of uncertain switched nonlinear systems," *IEEE Transactions on Fuzzy systems*, vol. 28, no. 4, pp. 632–644, 2019.

[13] T. Takagi, "Fuzzy identification of systems and its application to modeling and control," *IEEE transactions on systems, man, and cybernetics*, vol. 15, no. 1, pp. 116–132, 1985.

[14] M.-J. Hu, J. H. Park, and Y.-W. Wang, "Stabilization of positive systems with time delay via the takagi–sugeno fuzzy impulsive control," *IEEE Transactions on Cybernetics*, vol. 52, no. 6, pp. 4275–4285, 2022.

[15] A. Benzaouia and R. Oubah, "Stability and stabilization by output feedback control of positive takagi–sugeno fuzzy discrete-time systems with multiple delays," *Nonlinear analysis: Hybrid systems*, vol. 11, pp. 154–170, 2014.

[16] I. Zare, P. Setoodeh, and M. H. Asemani, "Fault-tolerant tracking control of discrete-time t-s fuzzy systems with input constraint," *IEEE Transactions on Fuzzy Systems*, vol. 30, no. 6, pp. 1914–1928, 2022.

[17] X. Xie, C. Wei, Z. Gu, and K. Shi, "Relaxed resilient fuzzy stabilization of discrete-time Takagi–Sugeno systems via a higher order time-variant balanced matrix method," *IEEE Transactions on Fuzzy Systems*, vol. 30, no. 11, pp. 5044–5050, 2022.

[18] K. Tanaka, H. Yoshida, H. Ohtake, and H. O. Wang, "A sum-of-squares approach to modeling and control of nonlinear dynamical systems with polynomial fuzzy systems," *IEEE Transactions on Fuzzy systems*, vol. 17, no. 4, pp. 911–922, 2008.

[19] M. Han, H.-K. Lam, F. Liu, Y. Tang, B. Han, and H. Zhou, "Stabilization analysis and impulsive controller design for positive interval type-2 polynomial fuzzy systems," *IEEE Transactions on Fuzzy Systems*, vol. 30, no. 9, pp. 3952–3966, 2022.

[20] B. Xiao, H. K. Lam, Z. Zhong, and S. Wen, "Membership-function-dependent stabilization of event-triggered interval type-2 polynomial fuzzy-model-based networked control systems," *IEEE Transactions on Fuzzy Systems*, vol. 28, no. 12, pp. 3171–3180, 2020.

[21] Z. Feng, Y. Yang, and H. K. Lam, "Extended-dissipativity-based adaptive event-triggered control for stochastic polynomial fuzzy singular systems," *IEEE Transactions on Fuzzy Systems*, vol. 30, no. 8, pp. 3224–3236, 2022.

[22] D. Zhang and B. Du, "Event-triggered controller design for positive t–s fuzzy systems with random time-delay," *Journal of the Franklin Institute*, 2022.

[23] J. M. Mendel, "Type-2 fuzzy sets and systems: An overview," *IEEE computational intelligence magazine*, vol. 2, no. 1, pp. 20–29, 2007.

[24] M. A. M. Rey, J. O. B. Blanco, and G. K. S. Paez, "An embedded type-2 fuzzy processor for the inverted pendulum control problem," *IEEE Latin America Transactions*, vol. 9, no. 3, pp. 240–246, 2011.

[25] M. A. Khanesar, E. Kayacan, M. Teshnehlab, and O. Kaynak, "Extended kalman filter based learning algorithm for type-2 fuzzy logic systems and its experimental evaluation," *IEEE Transactions on Industrial Electronics*, vol. 59, no. 11, pp. 4443–4455, 2011.

[26] R. H. Abiyev and O. Kaynak, "Type-2 fuzzy neural structure for identification and control of time-varying plants," *IEEE Transactions on Industrial Electronics*, vol. 57, no. 12, pp. 4147–4159, 2010.

[27] H. K. Lam and L. D. Seneviratne, "Stability analysis of interval type-2 fuzzy-model-based control systems," *IEEE Transactions on Systems, Man, and Cybernetics, Part B (Cybernetics)*, vol. 38, no. 3, pp. 617–628, 2008.

[28] X. Zhao, Y. Yin, B. Niu, and X. Zheng, "Stabilization for a class of switched nonlinear systems with novel average dwell time switching by t-s fuzzy modeling," *IEEE Transactions on Cybernetics*, vol. 46, no. 8, pp. 1952–1957, 2015.

[29] Z. Li, H. Yan, H. Zhang, H. K. Lam, and M. Wang, "Aperiodic sampled-data-based control for interval type-2 fuzzy systems via refined adaptive event-triggered communication scheme," *IEEE Transactions on Fuzzy Systems*, vol. PP, no. 99, pp. 1–1, 2020.

[30] H. K. Lam, "A review on stability analysis of continuous-time fuzzy-model-based control systems: From membership-function-independent to membership-function-dependent analysis," *Engineering Applications of Artificial Intelligence*, vol. 67, pp. 390–408, 2018.

[31] X. Li, H. K. Lam, F. Liu, and X. Zhao, "Stability and stabilization analysis of positive polynomial fuzzy systems with time delay considering piecewise membership functions," *IEEE Transactions on Fuzzy Systems*, vol. 25, no. 4, pp. 958–971, 2017.

[32] X. Li, K. Mehran, and Z. Bao, "Stability analysis of discrete-time polynomial fuzzy-model-based control systems with time delay and positivity constraints through piecewise taylor series membership functions," *IEEE Transactions on Systems, Man, and Cybernetics: Systems*, vol. 51, no. 12, pp. 7517–7529, 2020.

[33] J. P. Boyd, "Defeating the runge phenomenon for equispaced polynomial interpolation via tikhonov regularization," *Applied mathematics letters*, vol. 5, no. 6, pp. 57–59, 1992.

[34] Z. Bao, X. Li, H. K. Lam, Y. Peng, and F. Liu, "Membership-function-dependent stability analysis for polynomial-fuzzy-model-based control systems via chebyshev membership functions," *IEEE Transactions on Fuzzy Systems*, vol. 29, no. 11, pp. 3280–3292, 2020.

[35] J. H. Holland, "Adaptation in natural and artificial systems," *University of Michigan Press*, 1975.

[36] J. Xiong, X. Liu, X. Zhu, H. Zhu, H. Li, and Q. Zhang, "Semi-supervised fuzzy c-means clustering optimized by simulated annealing and genetic algorithm for fault diagnosis of bearings," *IEEE Access*, vol. 8, pp. 181 976–181 987, 2020.

[37] X. Li, H. K. Lam, G. Song, and F. Liu, "Stability analysis of positive polynomial fuzzy-model-based control systems with time delay under imperfect premise matching," *IEEE Transactions on Fuzzy Systems*, vol. 26, no. 4, pp. 2289–2300, 2017.

[38] H. K. Lam, H. Li, C. Deters, E. L. Secco, H. A. Wurdemann, and K. Althoefer, "Control design for interval type-2 fuzzy systems under imperfect premise matching," *IEEE Transactions on Industrial Electronics*, vol. 61, no. 2, pp. 956–968, 2013.

[39] M. J. D. Powell *et al.*, *Approximation theory and methods*. Cambridge university press, 1981.

[40] A. Lipowski and D. Lipowska, "Roulette-wheel selection via stochastic acceptance," *Physica A: Statistical Mechanics and its Applications*, vol. 391, no. 6, pp. 2193–2196, 2012.

[41] M. Meng, J. Lam, J. Feng, X. Zhao, and X. Chen, "Exponential stability analysis and l1 synthesis of positive t-s fuzzy systems with time-varying delays," *Nonlinear Analysis Hybrid Systems*, vol. 24, pp. 186–197, 2017.